Abstract

Analysis of *scn5Laa* and *scn5Lab* Gene Function in *Danio rerio* (Zebrafish) Heart Development through TALENs/CRISPR-CAS9-mediated Gene Knockout

Payal Chokshi

17 April, 2015

Director of Thesis: Edmund J. Stellwag, Ph.D.

Department of Biology

Research in our laboratory is focused on understanding the molecular developmental genetic effects of crude oil exposure on vertebrate embryogenesis. Our research has demonstrated that exposure of zebrafish embryos to crude oil results in characteristic developmental anomalies marked by pericardial edema, progressive deterioration of the developing heart and cardiac stasis coupled with larval death (Ghiassi, 2014). Chopra et al. observed very similar developmental defects after antisense oligonucleotide (MO)-mediated knockdown of the voltage-gated sodium ion channel genes *scn5Laa* and *ab* (Chopra et al. 2010). They further demonstrated that the developmental defects induced by the zebrafish *scn5Laa* and *ab*-directed MO's acted independently of their effects as ion channel disrupters, indicative that the *scn5Laa* and *ab* gene-encoded proteins have separate ion channel and developmental functions. Since knockdown of zebrafish *scn5Laa* and *ab* induce defects that effectively phenocopy the teratogenic effects of crude oil in the zebrafish model, we wanted to

verify that the *scn5Laa* and *ab* genes function in normal zebrafish heart development. Since MO-mediated gene knockdown phenotypes are often associated with off-target MO activities, verification of the activity of these genes in development required gene knockouts. Therefore, the aim of this research was to create zebrafish *scn5Laa* and *scn5Lab* gene knockouts using both TALENs and CRISPR-CAS9 gene editing methods and to determine whether these knockout mutants mirror the phenotypes observed by Chopra et al. (Chopra et al. 2010). Assuming that the effects of MO's on translation of *scn5Laa* and *scn5Lab* gene-derived mRNA are specific and results in gene knockdowns that directly affect embryonic heart development, we hypothesized that the zebrafish *scn5Laa* and *ab* gene knockouts would generate developmental defects similar to those reported by Chopra et al. (Chopra et al. 2010). To test our hypothesis, we created homozygous zebrafish *scn5Laa and ab* frameshift mutants using both TALENs and CRISPR-CAS9 gene editing methods. Screening of independent homozygous *scn5Laa* and *scn5Lab* frameshift mutant alleles for developmental defects, failed to demonstrate an increase in embryos with defects above frequencies observed among appropriate wild-type zebrafish controls. Since Chopra et al. (2010) observed stereotypical development heart defects among zebrafish treated independently with MO's directed toward either *scn5Laa* or *scn5Lab* genes, we reject the hypothesis that independent *scn5Laa* or ab gene knockout can generate mutants with developmental heart defects that mirror those induced by MO's. The absence of developmental heart defects among zebrafish bearing frameshift mutations in either *scn5Laa* or ab suggest that these genes act independently are not responsible for specification of normal zebrafish heart development. It is, however, possible that the absence of a detectable heart defect

among knockout mutants may reflect the fact that both paralogs are required for normal heart specification and that Chopra et al.'s (2010) MO treatment with individual MO's simultaneously affected the expression of both genes. If so, then double knockouts of *scn5Laa* and ab would be required to recapitulate the heart developmental defects reported by Chopra et al. (2010). It is also possible that other members of the Na^+ ion channel family proteins are required for normal heart development and that Chopra et al.'s MO knocked down their activities sufficiently to induce developmental heart defects. If so, additional gene knockouts for additional members of the Na^+ ion channel family genes would have to be constructed and tested separately or in combination to test this hypothesis. It is also possible that the Chopra et al. results were attributable to widely acknowledged MO off-target, non-specific effects. Future experiments including the screening of *scn5Laa* and ab double mutants, will provide information about whether both genes are required to specify normal heart development and whether the results reported by Chopra et al (2010) were related to simultaneous knockdown of *scn5a* paralogs by single MOs.

Analysis of *scn5Laa* and *scn5Lab* Gene Function in *Danio rerio* (Zebrafish) Heart Development through TALENs/CRISPR-CAS9-mediated Gene Knockout

A Thesis

Presented To the Faculty of the Department of Biology

East Carolina University

In Partial Fulfillment

Of the Requirements for the Degree

Master of Science in Molecular Biology/Biotechnology

By

Payal Chokshi

17 April, 2015

Analysis of *scn5Laa* and *scn5Lab* Gene Function in *Danio rerio* (Zebrafish) Heart Development through TALENs/CRISPR-CAS9-mediated Gene Knockout

By

Payal Chokshi

APPROVED BY:

DIRECTOR OF THESIS: _____
Edmund J. Stellwag, Ph.D.

COMMITTEE MEMBER: _____
Yong Zhu, Ph.D.

COMMITTEE MEMBER: _____
Anthony A. Capehart, Ph.D.

COMMITTEE MEMBER: _____
Barbara Muller-Borer, Ph.D.

CHAIR OF THE DEPARTMENT
OF BIOLOGY: _____
Jeffrey S. McKinnon, Ph.D.

DEAN OF THE
GRADUATE SCHOOL: _____
Paul J. Gemperline, Ph.D.

DEDICATION

To my parents, siblings, and fiancé:

Thank you for your constant love, support, and courage to help me grow and be the person who I am today.

ACKNOWLEDGEMENT

Biotechnology and genomic engineering are not easy tools to grasp and master. This project would not have been possible without some of the most talented scientists at East Carolina University. First, I would like to thank my thesis mentor, Dr. Edmund Stellwag for believing in me and giving me the opportunity to learn and discover more about biotechnology. His brilliant mind, support, and understanding on genetics is invaluable.

Second, I would like to thank one of my most valuable committee members, Dr. Yong Zhu. Dr. Zhu has taught me most of the genomic engineering techniques, while increasing my interest in science throughout my graduate years. He is the most dedicated and hardworking scientist I have ever met. This project would not have been possible without Dr. Zhu's incredible knowledge and guidance. In addition, I would like to thank my two other committee members, Dr. Anthony Capehart and Dr. Barbara Muller-Borer. I appreciate the guidance, support, and time you have put into me and in this project throughout the years. Your exceptional knowledge and input is a big part of this project.

My sincere thanks to two of my fellow graduate students, Lengxob Yong and Zoe Shaner. While working on projects that both employ genome editing techniques, Lengxob and Zoe provided useful technical and conceptual help and advice with the project. I could not thank them enough for their constant help and support throughout my graduate career.

Last but not least, I would like to thank all my undergraduate students: Connie Lutz, Kaeden Jordison, Zayer Thet, Leah Taylor, Christopher Allen, Nichole Carter,

Peter Soares, and Aaron Hyman. Their help with keeping all of our mutants healthy, alive and keeping the fish laboratory clean and organized is greatly appreciated. Connie, Kaeden, and Zayer have gone above and call of duty to contribute to this project. They helped with all the physiological characterization experiments, mutant screening and many of the genetic crosses. Leah, Chris, Peter, and Aaron also helped greatly with the physiological characterization of the zebrafish mutants and genetic crosses. This project would not have been successful if I had not gotten additional help from all of my undergraduate students. I sincerely thank you all for being a part of our lab and could not be more proud of you.

TABLE OF CONTENTS

LIST OF TABLES

LIST OF FIGURES

LIST OF ABBREVIATIONS

3’	3 prime end of a DNA Strand
5’	5 prime end of a DNA strand
α	Alpha
A	Alanine
aa	Amino acid
AMP	Ampicillin
β	Beta
bp	base pair
BP	British Petroleum
°C	Degree Celsius
Cas	CRISPR-CAS9 Associated Protein System
CRISPR-CAS9	Clustered Regularly Interspaced Short Palindromic Repeats
crRNA	CRISPR-CAS9 RNA
D	Aspartic Acid
DH5α	Strain of *E.coli* used for cloning
DI-DIV	Domain I to Domain IV
DNA	Deoxyribonucleic Acid
dNTPs	Deoxynucleotide triphosphate
dpf	Days post-fertilization
DSBs	Double stranded breaks
E	Glutamic acid

EDTA	Ethylenediaminetetraacetic acid
F0	Parental generation
F1	First generation
F2	Second generation
F3	Third generation
Fw	Forward
G	Glycine
gRNA	Guide RNA
H	Histidine
HD	Histidine and Aspartic Acid
hpf	Hours post-fertilization
I	Isoleucine
Indel	Insertion or deletion
IPTG	Isopropyl β-D-1-thiogalactopyranoside
K	Lysine
kb	Kilo bases
kDa	Kilo Dalton
LB	Lysogeny Broth for bacteria growth
LQTS	Long Q-T Syndrome
M	Molar
MC 252	Macondo 252 crude oil
Met	Methionine
$Mgcl_2$	Magnesium Chloride

Min	Minute
ml	Milliliter
mM	MilliMolar
MO	Antisense morpholino oligonucleotide
mRNA	Messenger ribonucleic acid
N	Asparagine
Na^+ ion	Positively-charged sodium ion
NaOH	Sodium hydroxide
NG	Asparagine and Glycine
NHEJ	Non homologous end joining
NI	Asparagine and Isoleucine
NN	Asparagine and Asparagine
pA	Plasmid targeting nucleotide adenine
PAM	Protospacer adjacent motif
pC	Plasmid targeting nucleotide cytosine
PCR	Polymerase chain reaction
pCS2-FokI	RVDs attached to FokI restriction endonuclease plasmid
pCS2-nCas9n	Cas 9 expressing plasmid
pCS2-PEAS	pCS2-FokI TALENs forward binding site
pCS2-PERR	pCS2-FokI TALENs reverse binding site
pG	Plasmid targeting nucleotide glycine
pGEM-T	a recombinant DNA vector-used for bacterial cloning
pL	Picoliter

pMD-TALE	Plasmid containing fully constructed RVDs
pMD18T	Single unit vector plasmid
PNK	Polynucleotide kinase
ppm	Parts per million
pT	Plasmid targeting nucleotide Thymine
pT7-gRNA	A recombinant DNA vector-used to express gRNA
RE	Restriction enzyme
RNA	Ribonucleic acid
rpm	Revolutions per minute
Rv	Reverse
RVD	Repeat variable di-residue
S1-S6	Six membrane spanning segments
SCD	Sudden cardiac death
SCN	Voltage gated sodium channel
Scn1A	Voltage gated sodium channel, Type I, α subunit
Scn2A	Voltage gated sodium channel, Type II, α subunit
Scn3A	Voltage gated sodium channel, Type III, α subunit
Scn5a	Voltage gated sodium channel, Type V, α subunit
Scn8A	Voltage gated sodium channel, Type VIII, α subunit
scn5Laa	*Scn5a*-like gene isoform A
scn5Lab	*Scn5a*-like gene isoform B

Sec	Second
sgRNA	Single guide RNA
SIDS	Sudden infant death syndrome
SNP	Single nucleotide polymorphism
TAL	Transcription activator like
TALE	Transcription activator like effector
TALENs	Transcription activator-like effector nucleases
tracrRNA	Trans-activating CRISPR-CAS9 RNA
μl	Microliter
μm	Micrometer
WT	Wild-type
X-Gal	5-bromo-4-chloro-3-indolyl-beta-D-galacto-pyranoside

Analysis of *scn5Laa* and *scn5Lab* Gene Function in *Danio rerio* (zebrafish) Heart Development through TALENs/CRISPR-CAS9-mediated Gene Knockout

CHAPTER 1: INTRODUCTION

Effect of crude oil exposure on vertebrate embryonic development

Despite the increasing number of environmental oil spills, especially the disastrous 2010 spill in the Gulf of Mexico, little is understood about the genetic and developmental effects of crude oil exposure on embryonic stage vertebrates. Based on this paucity of information, our laboratory has been examining the developmental response of zebrafish embryos to crude oil exposure to determine if there are characteristic developmental defects and, if so, to characterize the underlying genetic and biochemical mechanisms leading to these defects.

Evidence from limited field and laboratory studies have shown that exposure of embryonic stage fish to crude oil results in major defects in jaw, pharyngeal arch, spine, craniofacial and heart development (Pauka et al. 2011; Machlis et al. 2010; Crone and Tolstoy 2010; Incardona et al. 2011; Incardona et al. 2004; Incardona et al. 2005; Carls et al. 2008; Carls et al. 1999; Heintz et al. 1999). The earliest and most readily identifiable defects are related to heart development and are manifested in field and laboratory studies by extreme pericardial edema followed by aberrant heart development marked by progressive wasting of the developing heart tissue, abnormal rhythms and reduced heart rate leading to cessation of the heart beating and blood circulation. Similar developmental defects have been demonstrated in embryonic stage fish after exposure to complex mixtures of polycyclic aromatic hydrocarbons, which

constitute a high percentage of the non-aliphatic hydrocarbons in crude oil (Hicken et al. 2011).

While the morphological defects induced by crude oil exposure in developing fish embryos are documented in both field and laboratory studies, little is known about the molecular nature of these defects. Based on gene expression and enzyme activity measurements, it has been determined that aryl hydrocarbon metabolizing enzymes and receptors are induced and that certain stress response pathways are elevated after exposure (Incardona et al. 2005; Nebert et al. 2004). However, the effects of crude oil exposure on genes involved in heart development and function are unknown.

Detailed stereomicroscopic studies of crude oil-treated zebrafish embryos conducted in our laboratory and similar studies by de Soysa et al. (2012) have shown that the embryonic heart develops abnormally during a protracted period beginning at about 48 hour post-fertilization and continuing through the larval stage of growth; terminating in larval death usually around 10-12 days post-fertilization (Ghiassi 2014; de Soysa et al. 2012). During this period the embryonic and larval heart appears to undergo progressive thinning of the atrial and ventricular walls with a failure to engage in characteristic looping and marked by continual reduction in heart rate (de Soysa et al. 2012). These morphological changes occur concurrently with continuous expansion of the pericardial sac leading to extreme pericardial edema, which suggests osmotic imbalance in the pericardium.

An examination of the zebrafish development literature revealed a number of mutants with defects in heart development similar to those observed after crude oil

treatment of embryos (Belaire et al. 2001; Henry et al. 1997). These include mutants that showed cardiac and yolk sac edema, cardiac arrhythmia, reduced larval heart rate and abnormal heart development. While these mutants are of significance because they suggest that single gene defects phenocopy the developmental heart defects induced by crude oil exposure, they have not been characterized genetically and so do not provide information about the specific gene expression or biochemical processes that could be affected by crude oil exposure. However, there is evidence from gene knockdown studies that a pair of gene paralogs that encode specific Na^+ ion channels-also phenocopy the developmental heart defects that have been observed after treatment of zebrafish embryos with crude oil (Chopra et al. 2010). A report by Chopra et al. (2010) showed that the independent or combined knockdown of either of two voltage gated Na^+ ion channel genes (*scn5Laa* and *scn5Lab*) using antisense morpholino oligonucleotides (MO) in zebrafish resulted in a phenocopy of the heart defects induced after crude oil exposure of embryos.

Expression studies using riboprobes directed toward these two genes show that they are expressed in the myocardium of the developing heart (Novak and Taylor et al. 2006). Treatment of embryos with Na^+ channel ion blocking agents that inhibited the ion channel activity of the *scn5Laa* and *ab*-encoded proteins failed to generate the heart development defects induced by the *scn5Laa* and *ab* MO-directed gene knockdown which suggests that these ion channels may have distinct functions both as ion channels and separately as factors required for normal heart development (Chopra 2008). While the results reported by Chopra et al. (2010) are indicative that the *scn5Laa* and *ab* gene-encoded protein products may be those that are affected by

crude oil exposure, MO-induced knockdown phenotypes are sometimes the product of MO-related toxicity or off-target effects (Chopra 2008). They could also arise because of MO-mediated knockdown of gene expression among genetically-related Na^+ ion channel protein family members. In order to ensure that the MO-induced phenotypes are authentic and specific, it is necessary to isolate gene knockouts for both of these genes to determine if *scn5Laa* and *Lab* gene knockout mutant's developmental phenotypes mirror those reported by Chopra et al. (2010).

Molecular Structure of zebrafish *scn5Laa* and *Lab* genes

In zebrafish, the voltage gated Na+ ion channel gene (*scn*) family is composed of eight alpha subunit genes and four beta (zβ1-zβ4) subunit genes (Novak et al. 2006; Chopra, Watanabe et al. 2007). In zebrafish, α subunit of *scn* genes are composed of four sets of duplicated genes called *scn1Laa* and *scn1Lab*, *scn4aa* and *scn4ab*, *scn5Laa* and *scn5Lab*, *scn8aa* and *scn8ab* (Novak et al. 2006). These genes in the *scn* family have high sequence similarities within the transmembrane repeat regions and ion channel coding regions. In addition, members of duplicated genes show higher similarities in their nucleotide and amino acid sequences (Novak et al. 2006). The *scn* family is unusual in zebrafish because all the duplicated genes have been retained since their divergence from a common ancestral gene. When duplicated genes are retained, it is usually because their functions diverge and the duplicates are both under selection or because the genes diverge and assume subfunctions of the original ancestral gene (Postlethwait et al. 2004). In either case, the evolutionary pathway of these gene duplicates, particularly the *scn5* paralogs, influence how these genes function relative to each other. In the case of duplicate subfunctionalized genes, one

might expect that expression occurs in different tissues of the same organ or different cell-types in the same tissue or regions. By contrast, if the genes diverged in function, they might be expressed and function differently in completely different tissues or cells.

Scn5Laa is located on chromosome 2 while *scn5Lab* is located on chromosome 24 in zebrafish (Kersey et al. 2013). The length of mature mRNA of *scn5Laa* is 5799 bp (accession # DQ149507) comprising 27 exons that span 6.6 kb (Figure 2) (Kersey et al. 2013). The mature mRNA length of s*cn5Lab* is 5865 bp (accession # DQ149508) containing 29 exons that span 6.5 kb (Figure 3) (Kersey et al. 2013). A comparison of the *scn5Laa* and *ab* transcripts shows that transcripts of *scn5Laa* are first expressed at 24hpf in the developing heart tube of zebrafish (Novak, Taylor et al. 2006), appear in the hind brain and mid-brain regions at 48 hpf and then throughout the rostral region of the nervous system by 60 hpf (Novak, Taylor et al. 2006). By comparison, the expression of *scn5Lab* mRNA transcripts are seen as early as 19 hpf in trunk somites, in spinal cord by 30 hpf, and a low expression in anterior and posterior lateral line nerves by 60 hpf (Novak, Taylor et al. 2006).

The primary protein structure of *scn5Laa* and *ab* gene-encoded proteins is 1932 amino acid long and 1954 amino acids, respectively. These genes encode proteins that form the α subunit of the Na^+ ion channels. The α subunit of sodium ion channel proteins is larger than that of the beta subunit comprising a ~240kDa protein with 24 membrane spanning domains compared to the β subunit typically a 30-40kDa protein "with a single transmembrane domain and an extracellular V-type immunoglobin-like domain (Chopra 2008)" (Isom et al. 1992; Isom et al. 1995; Morgan et al. 2000; Yu et al. 2003; Isom and Catterall 1996). The tertiary structure of a typical voltage gated sodium

channel includes four homologous domains called DI-DIV (Figure 1). Each of these domains are comprised of six membrane spanning segments S1-S6 (Marban et al. 1998; George Jr. 2005; Roden et al. 2002). Segments S5-S6 predominantly forms the pore's channel (Figure 1). Evidence from biophysical studies show that the residues D(DI), E(DII), K(DIII), A(DIV) specify each channel's ion selectivity (Sun et al. 1997). Domains III and IV forms an intracellular linker that acts as an ion inactivation gate to form ion permeable pathways into the membrane during repolarization state (Figure 1). The S4 transmembrane segment is comprised of charged residues of arginine or lysine at every third position and are suspected to play a significant role in depolarization to open the channels (Figure 1) (Sun et al. 1997). In the tertiary structure of α subunit, the four homologous domains are predicted to form a fourfold symmetry surrounding S5-S6 interlink dipping down into the membrane forming a central pore (Lehmann-Horn and Jurkat-Rott 1999). The S1-S3 segments are thought to reside near the lipid bilayer because of their amphipathic nature to interact with polypeptides and lipids (Guy and Durell 1995) while S5-S6 segments are located near the central pore establishing a narrow selectivity filter. The S4 segment is believed to move outward (away from the central pore) during the depolarizing stage (Guy and Durell 1995). The quaternary structure is established when the pore forming α subunit binds to one or more β subunits. Additional quaternary arrangements of the Na^+ ion channels vary depending on the binding of the α and β subunits to various other proteins that determine membrane localization, voltage sensitivity and connectivity (Gurnett and Campbell 1996).

In mammals, the voltage gated Na+ ion channel gene family is composed of 10 distinct α subunit *SCN* genes (*SCNxA*) and 4 distinct β subunit genes (*SCN1B-SCN4B*) (Yu and Catterall 2003; Goldin 2001; Catterall et al. 2005). Genes *scn5Laa* and *scn5Lab* are highly similar to mammalian *SCN5A* gene-encoded protein, primarily found in cardiac tissues (Rogart et al. 1989). The expression of *scn5Laa* and *scn5Lab* are not just limited to cardiac tissue but are also found in skeletal and nervous system. Moreover, biochemical and physiological evidence suggests that zebrafish sodium channel genes are likely to be conserved in function and structure with mammalian sodium channel genes (Baker et al. 1997; Ribera and Nusslein-Volhard 1998; Tsai et al. 2001; Warren et al. 2001). According to Chopra, *scn5Laa* shows 76.1% identity and 82.8% similarities with *scn5Lab* and both of these genes show roughly 60% amino acid similarities to human *SCN5A* (Chopra 2008).

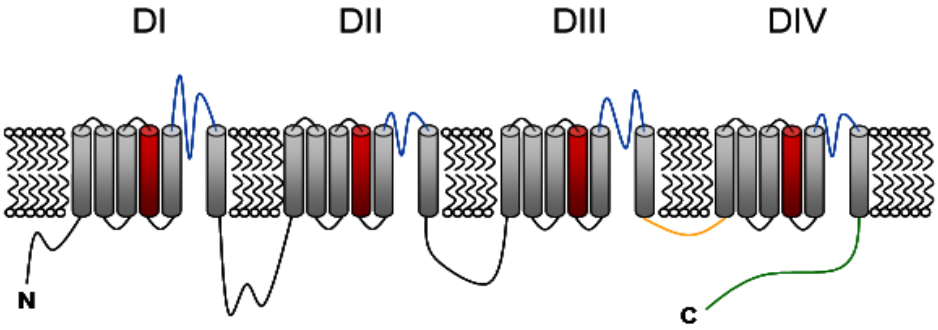

Figure 1: Secondary structure of a typical voltage-gated sodium channel (from Chopra, 2008) Voltage-gated sodium channels are comprised of 4 homologous domains, each with 6 membrane-spanning segments. Among the functionally-important regions of the channel are the S4 voltage sensors (red), which have basic residues at every third position and act to transduce changes in membrane potential into movement of the channel; the pore loops (blue), comprised of the linkers connecting the S5 and S6 transmembrane segments within each domain and which contain the channel's

selectivity filter (D-E-K-A); the fast inactivation gate (orange), which is the intracellular linker connecting domains III and IV that acts to plug the ion permeation pathway after depolarization; and the C-terminus (green), which has calcium-binding EF hand structures and motifs for interaction with diverse proteins.

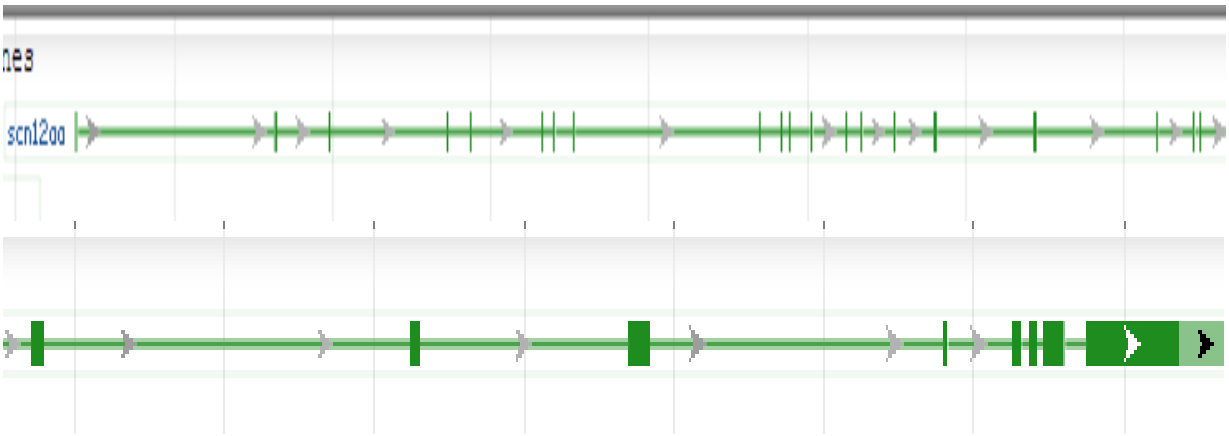

Figure 2: Exon/intron structure of *scn5Laa* located on chromosome 2 (Accession #DQ149507) Vertical lines in darker green color represent exons. The region between each exon represents introns. The arrows represent the direction from the start of the exon to the end of the exon.

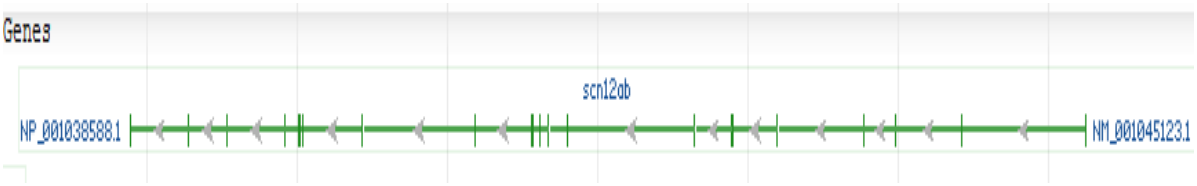

Figure 3: Exon/intron structure of *scn5Lab* located on chromosome 24 (Accession #DQ149508) Vertical lines in darker green color represent exons. The region between each exon represents introns. The arrows represent the direction from the start of the exon to the end of the exon.

Functional Redundancy of Gene Paralogs

Phylogenetic evidence suggests that *scn5Laa* and *scn5Lab* are gene duplicates that likely arose from a single ancestral gene as part of a whole genome duplication event that occurred early in teleost evolution. Gene duplicates that have diverged evolutionarily can express functional redundancy, either complete or partial, as mutations accumulate and drive the protein products to divergent but overlapping function. This process of divergence with retention of overlapping function is referred to as subfunctionalization, a process that has been documented for duplicate gene paralogs (Lambert et al. 2015; Kawaguchi et al. 2013). Overlapping expression patterns of *scn5Laa* and *ab* during embryonic development of the heart are indicative of subfunctionalization and suggest that these two genes may act together to specify normal heart development. In addition to the likely possibility that *scn5Laa* and *ab* are functionally redundant, there is evidence that members of the Na^+ channel protein family are related and have overlapping subfunctions (Watanabe et al. 2000). Depending on the extent of functional redundancy expressed by *scn5Laa* and *ab*, it is possible that knocking out either *scn5Laa* or *scn5Lab* alone might not produce the defective developmental cardiac phenotype observed by Chopra et al. following MO knockdowns (Chopra et al. 2010).

A comparison of the exon-intron structure of *scn5Laa* and *scn5Lab* shows that they are 76.1% similar in identity and 82.8% in similarity (Chopra 2008). Further comparisons of amino acid sequences of *scn5Laa* and *scn5Lab* shows that they are highly similar in the domains that encode transmembrane region and ion channels. Six (S1-S6) transmembrane regions (Marban et al. 1998; George Jr. 2005; Roden et al.

2002) span each of the four domains (I-IV) in both *scn5Laa* and *ab*. Specifically the S4 transmembrane region plays an important part in action potential. In both of these genes, transmembrane segments S5 and S6 contains a pore loop (Figure 1) that acts as a selectivity filter (Chopra 2008). The inactivation gate is located intracellularly and linked between domains III and IV. The extracellular loop between domain I and II are coded by exons 9 and 10 of both *scn5Laa* and s*cn5Lab*; whereas, the extracellular loop between loop II and III are coded by exons 14 and 15 of both *scn5Laa* and *ab* (Novak et al. 2006). These extracellular loops play a role in ion permeable pathways during the depolarization stage.

Human *SCN5A* alleles: Correlation with heart defects

SCN5A found in humans and other mammals is highly expressed in mature myocardium and is required for cardiac contractions. Mature *SCN5A* mRNA product contains 28 exons (Wang et al. 1996). Evidence reported in the literature shows that mutation in *SCN5A* leads to various cardiac diseases such as Brugada syndrome, long Q-T syndrome (LQTS), atrial standstill, congenital sick sinus syndrome, progressive cardiac conduction system, and sudden infant death syndrome (SIDS) (George Jr. 2005; Koopmann et al. 2006). Rare mutations found in *SCN5A* can disrupt cardiac arrhythmia and lead to Brugada syndrome, LQTS and eventually sudden cardiac death (SCD) (Marban 2002; Vincent 1998). SCD was the leading cause of mortality in The United States in 1998 causing 300,000 deaths (Zipes and Wellens 1998).

Brugada syndrome is usually inherited from families in autosomal dominant manner and is caused by missense, nonsense, splicing, and frameshift mutations

throughout *SCN5A* coding regions. *SCN5A* mutation causing Brugada syndrome is perceived by right bundle branch block which causes loss of sodium channel function in mutant channels to the cell membrane leading to reduction is sodium channel availability and trafficking (Wang et al. 2000; Balser 1999; Valdivia et al. 2004; Herfst et al. 2004). Evidence of the literature suggests that a G-to-T missense mutation at position 4372 was predicted to change the amino acid glycine for an arginine (G1406R) between the S5 and S6 transmembrane segment of DIII domain (Kyndt et al. 2001). Patients evaluated with this missense mutations showed cardiac conduction defects and Brugada phenotype, which required cardioverter-defibrillator implants in one patient (Kyndt et al. 2001). Furthermore, another patient with missense mutation leading to substitution of a valine instead of a glycine (G352V) coding for transmembrane segment S5 and S6 in domain DI led to Brugada syndrome (Vatta et al. 2002). A 20 bp deletion in exon 5 of *SCN5A*, which codes for part of transmembrane S2 and S3 of DI was also linked to Brugada phenotype (Vatta et al. 2002). In addition, substitution of amino acid lysine by glutamic acid (K126E) at DI-S1 boundary in the intracellular loop was also connected to Brugada syndrome (Vatta et al. 2002).

Similar missense mutations leading to substitution of arginine to histidine (R689H) resulted in a loss of function even in heterozygous individual leading to both Brudaga syndrome and LQTS (Hong et al. 2012). LQTS represents longer Q-T interval, frequent syncope, and SCD due to tachycardia (Moss 2003) and is known to be linked to defects in *SCN5A* and other ion regulating genes (Wang et al. 1995; Mohler et al. 2003). LQTS can lead to sudden death syndrome in a healthy heart. *SCN5A* missense

mutations linked to the non-synonymous amino acid substitution leading to R1193Q, N1325S, R1644H occur in LQTS patients (Wang et al. 2004).

Transgenic studies in mice with targeted deletion in the *SCN5A* gene lacking sequences coding for amino acid residues 1505-1507 (KPQ) and separate experiments that knockouts in LQTS mutant alleles from the human *SCN5A* gene both showed polymorphic ventricular arrhythmias and slow conduction, ventricular tachycardia, sinus node dysfunction, increased refractories, respectively (Nuyens et al. 2001; Papadatos et al. 2002; Lei et al. 2005). These studies further reported embryonic lethality of the homozygous mice with targeted deletions suggesting an important role of *SCN5A* in cardiac development. Furthermore, these studies reported that heterologous expression of *SCN5A* mutation leading to LQTS do not inactivate sodium channel but rather leads to sustain depolarization stage during plateau phase of action potential (Wang et al. 1996; Keating 1996; Dumaine et al. 1996). This evidence suggests that mutation in *SCN5A* leads to reduction in sodium current which might increase sodium channel blocking arrhythmia (Pu et al. 1998; Liu et al. 2002; Balser 2001; Viswanathan et al. 2001; Shimizu et al. 2000).

A recent study reporting the construction of transgenic zebrafish bearing an integrated copy of the human *Scn5a-D1275N* allele gene showed that the fish developed bradycardia, conduction system abnormalities, and pre mature death even though these fish carried wild-type alleles for *scn5Laa* and *ab* (Huttner et al. 2013). These findings suggest that *SCN5A* can act as a dominant negative gene since expression of human *Scn5a-D1275N* allele lead to defective cardiac function and

embryonic death even in the presence of wild-type *scn5Laa* and *scn5Lab* (Huttner et al. 2013).

TALENs and CRISPR-CAS9 Genome editing*: scn5Laa* and *ab* gene knockouts

TALENs are novel proteins that are used in gene editing to target specific DNA sequences for introduction of sequence-specific mutations by inducing sequence-specific double strand breaks (DSBs). The DSBs generated by the action of TALENs proteins commonly generate insertion or deletion (indel) mutations through the action of an endogenous cell non-homologous end joining (NHEJ) DNA repair mechanism (Cade et al. 2012). TALENs are composed of a non-binding non-specific Type IIS *FokI* endonuclease domain fused to a highly conserved DNA binding domain derived from transcription activator-like (TAL) effectors (Cade et al. 2012). The highly conserved DNA binding domain is composed of repetitive 33-35 amino acid repeats. Evidence from the literature states “Individual TALE repeats in an array specifically bind to a single base of DNA, the identity of which is determined by two hypervariable residues typically found at positions 12 and 13 of the repeat” (Joung and Sander p.50). Thus, variable di-residues at positions 12 and 13 determine the nucleotide base a particular TALE repeat-will bind to and target for *FokI* endonucleolytic cleavage. For example, asparagine (N) and glycine (G) at the position 12 and 13 of the repeat variable di-residue (RVD) is known to target the nucleotide thymine as shown in Figure 4. Similarly, at position 12 and 13, di-residues histidine (H) and aspartic acid (D), asparagine (N) and isoleucine (I), asparagine (N) and asparagine (N) target nucleotides cytosine, adenine, or guanine, respectively (Figure 4). Since TALENs function as dimers, assembling TALENs requires construction of a forward TALE binding site, a spacer region, and a reverse TALE

binding site (Huang et al. 2011). Usually, left and right binding sites of the TALENs are from 16-21 nucleotides long and the spacer region ranges from 14-17 nucleotides in length (Dahlem et al. 2012). When TALENs bind to the targeted sites, they induce DNA double-stranded breaks into the spacer region via the action of *FokI* restriction endonucleases activity that is expressed as a fusion protein with each TALENs. Genomic target sites for TALENs-induced DSB breakage are mostly chosen closer to 5' end of the gene sequence with the intention of inducing indel mutations that will result in-frameshift mutations early in the coding sequence. Frameshifts early in the gene's mRNA coding sequence increase the probability of generating translational terminators that result in substantial reduction or complete inactivation of the protein's function (Dahlem et al. 2012). TALENs are used in this study because the RVDs can be assembled to target any sequence starting with 5' T, which provides considerable latitude in targeting gene sequences (Cade et al. 2012; Reyon et al. 2012).

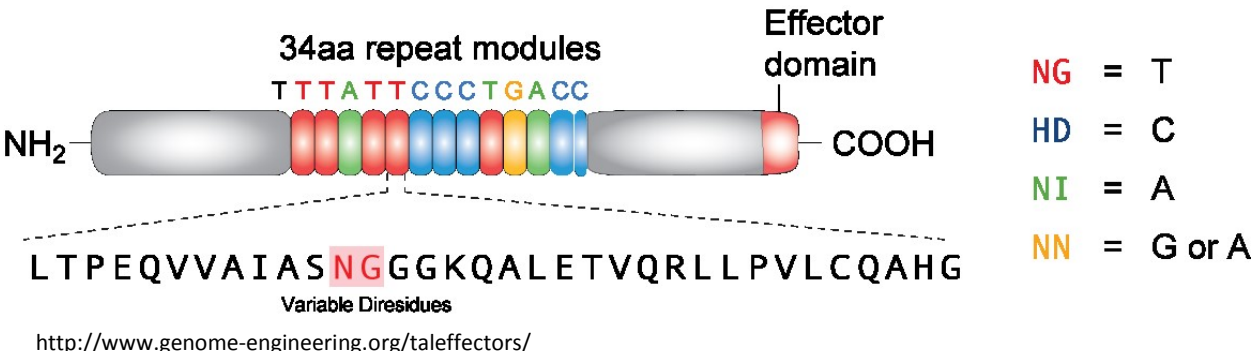

Figure 4: 34 Aminoacid repeats. Position 12 and 13 show variable di residues
Note: Diresidues NN also has specificity for A along with G. This can create a major problem for binding specificity.

Sequence-specific genome editing can also be achieved using the CRISPR-CAS9 editing system. The type II CRISPR-CAS9 system is composed of Cas 9 endonuclease, two small RNAs called CRISPR-CAS9 RNA (crRNA) and trans-activating CRISPR-CAS9 RNA (tracrRNA). A recent study discovered that a single guide RNA (gRNA) can substitute for the crRNA:tracrRNA complex and recruit Cas 9 protein to the target site on DNA (Jinek et al. 2012). Because gRNA can recruit Cas 9 protein to specific target sites on DNA, the only customized component needed for induction of double stranded DNA breaks is gRNA. Thus, the CRISPR-CAS9 system is simple, more cost effective, less time consuming and more efficient in the generation of germ-line mutations compared to TALENs. The CRISPR-CAS9 target site is optimally 23 bp long (Figure 5). The gRNA can be designed toward any target sequence provided that the sequence conforms to the following general structure 5'-GG-N18-NGG-3' (Jao et al. 2013). As a result, it is relatively simple to design gRNA complementary to any sequence starting with 5'-GG and ending with PAM sequence (NGG) (Hwang et al. 2013).

Both TALENs and CRISPR-CAS9 genome editing were used to create sequence-specific knockouts within both zebrafish *scn5Laa* and *ab* genes to determine whether these genes individually play a role in the specification of embryonic heart development as concluded by Chopra et al. based on the result of MO knockdown experiments (Chopra et al. 2010) If zebrafish *scn5Laa* and *ab* function in specification of embryonic heart development, then we hypothesized that TALENs and CRISPR-CAS9 generated knockout mutant null alleles will show developmental phenotypic defects that mirror those by resulting from independent MO-induced knockdown of

these genes. Further, based on defective heart function and premature death phenotype of a zebrafish transgenic line with a stably integrated allele of the human *SCN5A* gene that predisposes humans to cardiac defects and premature death, we further hypothesized that zebrafish *scn5Laa* or *ab* knockouts may exhibit embryonic lethality even in a heterozygous condition.

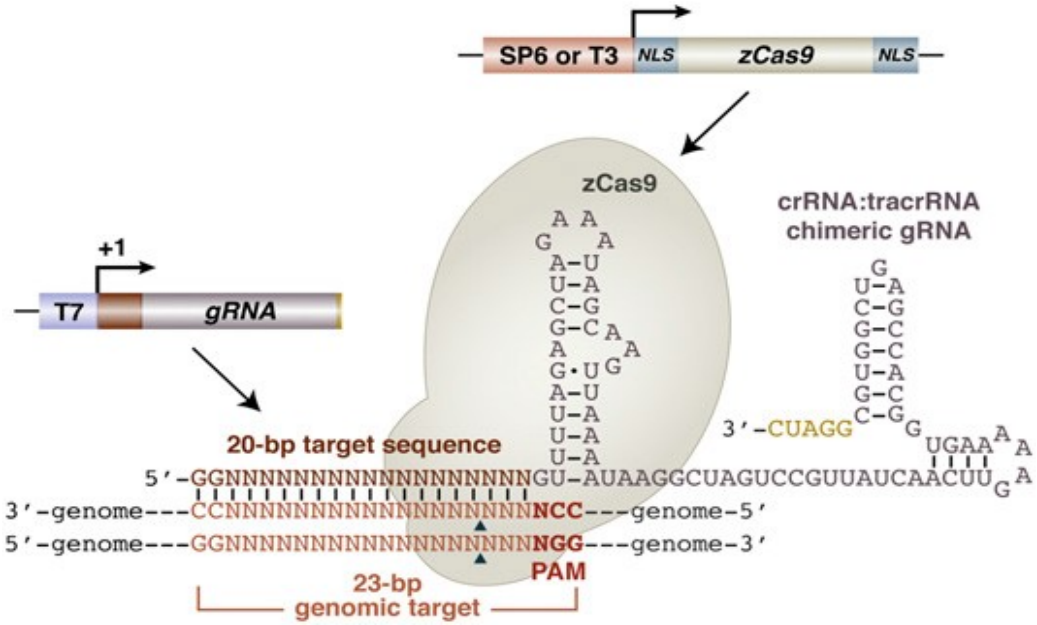

Figure 5: Schematic diagram of CRISPR-CAS9 system containing Cas 9 and crRNA:tracrRNA (Jao et al. 2013)gRNA attract Cas9 endonuclease to the targeted site. Cas9 induces DNA double stranded breaks 3 bp upstream of PAM sequence.

CHAPTER 2: METHODS

TALENs-based genome editing mutagenesis

Nucleotide sequences of the *scn5Laa* and *scn5Lab* genes were obtained from NCBI ("Using Pubmed") using accession numbers DQ149507 and DQ149508, respectively. The sequences of exons for these genes were found using Ensemble genome browser (Kersey et al. 2013). For *scn5Laa*, the TALENs target site was located in exon 7. The forward targeted site was 17 base pairs (bp) long consisting of nucleotides CAGTGTCTTCGCTCTGA; similarly, the reverse targeting site was also 17 bp long containing nucleotides GTCTCAGGATCCCCATG. The spacer region between the forward and reverse TALENs targeting sequences was 16 bp long (TCGGTCTGCAGCTCTT). For *scn5Lab*, the TALENs target site was located in exon 5. The forward, 17 bp target site contained nucleotides CCTGGCGCGGGGTTTCT; whereas, the reverse, 19 bp nucleotides were TCCAGGGGTCCCTCAGAAA. The spacer region was 17 bp long containing nucleotides GCATCGGGCCCTTCACA. To construct RVDs (repeat variable di-residues) the following steps were used.

Initially, five different single unit vectors (pMD18T) called pA, pT, pG, pC, corresponding to RVD NI, NG, HD, NN were used to provide individual repeats (Huang et al. 2011). The size of the single unit vector was 2807 bp as shown in Figure 6. In order to construct vectors containing RVDs in a particular order and number, repeated digestion/ligation cycles were used. For example, to construct RVD pA and pT joined together, pA and pT were double digested together with restriction enzymes shown in Table 1. pA was treated as a vector and pT was treated as an insert (Huang et al. 2011). The samples were incubated at 37°C for 2-4 hours to allow complete digestion.

Gel extraction was used to obtain digested pA and pT (note: 1% agarose gel was used unless otherwise specified). The QIAquick gel extraction kit and protocol was used to purify digested and electrophoresed DNA from both the digested vector and insert. Next, pA and pT DNA were ligated by using the reagents shown in Table 2 and incubated at room temperature for 30 minutes to 1 hour (Figure 7) (Huang et al. 2011). After ligation, 5 μl of ligation mixture was used to transform 50 μl of DH5α *E. coli* competent cells (Note: DH5α *E. coli* competent cells were used for transformation process in this entire experiment). A total 55 μl of the competent cells plus ligation mixture was incubated on ice for 30 minutes, then the sample was "heat shocked" at 42°C for 90 seconds. Immediately after the heat shock, the sample was transferred back to ice for 2 minutes. Then 250 μl of LB/AMP was added to the ligation mixture. The Eppendorf tube containing heat shocked *E. coli* treated with ligation mixture was then shaken at 37°C at 225 rpm for 45 minutes to 1 hour. The competent cell suspension was plated on an LB/AMP plate and incubated at 37°C for a minimum of 12 hours (Huang et al. 2011).

Recombinant DNA containing clones were assayed for inserts by PCR based screening using the reagents shown in Table 3. PCR amplification of DNA extracted from recombinant containing clones was conducted for 30 cycles. Primers M13-47 and RV-M corresponding sequences 5'-CGCCAGGGTTTTCCCAGTCACGAC-3', and 5'-AGCGGATAACAATTTCACACAGGA-3', respectively were used for PCR (Huang et al. 2011). The PCR product was electrophoresed on a gel to visualize positive clones by using a reference marker of 204bp for 2 unit assembly. Transformants containing inserts with the correct number and orientation of repeat sequences were grown in ~7-8

ml of LB/AMP at 37°C for 19-22 hours at 275 rpm in order to prepare a sufficient quantity of DNA for subsequent cloning. Plasmid DNA was purified from cells using QIAprep spin miniprep kit according to the manufacturer's protocol. In order to add additional RVD repeats, the procedure above was repeated by adding dimer repeats to the existing backbone using the appropriate inserts until the complete number and order of TALE repeats with the correct targeting sequence was achieved (Figure 8) (Huang et al. 2011). The fully constructed molecule was designated pMD-TALE plasmid. The sequence of the completed insert was verified by sequencing using the same primers used for PCR (M13-47 and RV-M) (Figure 9).

RVD repeats were cloned into pCS2-FokI (Figure 10) plasmid vectors including pCS2-PEAS (to generate left binding site) and pCS2-PERR (to generate right binding site) (Huang et al. 2011) and the FokI-TALENs fusion gene. Both pCS2-PEAS and pCS2-PERR plasmids were digested with NheI (to linearize) and de-phosphorylated after digestion (Huang et al. 2011). pMD-TALE plasmid (treated as an insert) was double digested with SpeI and NheI (Figure 11) and ligated to either the pCS2-PEAS or pCS2-PERR vector. Ligation products were transformed into DH5α *E. coli* competent cells as described above and the cells were plated on LB/AMP plates and incubated overnight. After selection of recombinant clones, cultivation, plasmid DNA extraction and purification, the TALE repeat sequence and orientation in the vector was confirmed via sequencing by using SP6 primer. The final constructed plasmids were designated PEAS-TALENs and PERR TALENs for forward and reverse TALENs targeting sites, respectively.

For *in vitro* transcription of the TALENs-FokI fusion gene in the plasmids PEAS-TALENs and PERR-TALENs for both *scn5Laa* and *scn5Lab*, NotI was used to linearize the plasmid, DNA was purified using a QIAprep column, and transcribed using a mMESSAGE mMACHINE SP6 kit. The transcribed mRNA was purified from the transcription reaction using RNeasy mini kit according to the manufacturer's protocol.

After successful *in vitro* transcription, zygotes or two cell embryos were microinjectioned with 500 pL to 1 nL of mRNA at a concentration of 300pg/nl at an injection with pressure (of the gas tank)13 psi, along with adjusting manually on microinjector apparatus Model PV 820 Pneumatic PicoPump (World Precision Instruments). At 48hpf after microinjections, DNA was extracted from 30 (WT and mutated) embryos by treating the embryos with 100 μl of 50mM NaOH solution for 30 minutes. The solution containing DNA was neutralized by adding 10μl of 1M Tris. PCR was performed on NaOH-extracted DNA using primers directed toward the target site on genomic DNA. After amplification, the presence of indel mutations was scored by digesting the PCR product using a restriction enzyme with a cleavage site unique to the spacer region of each gene, either *scn5Laa or scn5Lab* (see Table 4). If there is no mutation present, the restriction enzyme would cleave the PCR fragment and to generate two separate fragments. However, since mutations alter the sequence of the restriction endonuclease cleavage site of the TALENs target, the recognition sequence of restriction enzyme would be altered and prevent digestion, resulting in a single fragment. Digested PCR amplification products were electrophoresed on a 2% agarose gel to screen for mutations (Figures 16 and 17). DNA fragments corresponding to restriction enzyme resistant products were gel purified using QIAquick gel extraction

protocol and ligated to the pGEM-T vector from Promega (Table 5). The ligation reaction was incubated at room temperature for ~1 hour before transformation. After ligation, 5 μl of the ligation reaction was used to transform 50 μl of competent DH5α *E.coli* cells using the same procedure as above except the LB/AMP plate was also plated with 100 μl of IPTG and 20 μl of X-Gal for blue white screening. Plated competent cells were grown overnight for at least 12-13 hours in a 37°C incubator. Between 8-10 recombinant clones were selected to grow in 7-8 ml LB/AMP broth medium for 19-20 hours in the shaker at 37°C and 275 rpm. Plasmid DNA from these cultures was purified using QIAprep column as described above and the DNA samples were sequenced using the T7 primer to screen for mutations.

CRISPR-CAS9 System-based genome editing mutagenesis

CRISPR-CAS9 target sites ($GGN_{18}GG$) for *scn5Laa* and *scn5Lab* were identified by locating a PAM sequence at the 3' end of the total 23bp target sequence. Using this approach, targeted sequences were identified in exons 5 and exon 2, respectively. The sites chosen were GGATTTCAGTGTCATCGTCATGG and GGCAGCCATACTGTTTCCACCGG for *scn5Laa* and *scn5Lab*, respectively. Forward and reverse oligonucleotides were obtained from Sigma Chem Co. (St. Louis, MO). Forward and reverse oligonucleotides were phosphorylated and annealed using the conditions shown in Tables 6a and 6b.

pT7-gRNA vector ("Chen and Wente Lab") was linearized by digesting with *Bgl*II and *Sal*I overnight at 37°C using the reagents shown in Table 7a. Then the digested product was purified using a QIAgen Column according to the manufacturer's instructions. Purified product was digested with *EP*SI (*Bsm*BI) overnight at 37°C using

the conditions shown in Table 7b. One μl of product was electrophoresed on a 1% agarose gel to verify linearization. After verification, the reaction was stopped by denaturing the enzyme at 80°C for 20 mins, the product was purified using QIAgen kit and DNA fragment prepared from annealed oligonucleotides were ligated to pT7-gRNA vector by using the conditions shown in Table 8. After successful ligation, *E. coli* DH5α cells were transformed using the same procedure as above. The clones with inserts were screened for the correct insert using T7 primer for DNA sequencing.

A Cas 9 expression plasmid pCS2-nCas9n, was also obtained from Chen and Wente labs ("Chen and Wente Lab"). Prior to transcription the plasmid was linearized using *Not*I and purified using a QIAprep column. Capped RNA were then synthesized using a mMESSAGE mMACHINE kit and purified using an RNeasy kit (Qiagen) according to the manufacturer's instructions (Jao et al. 2013). The mix of Cas 9 RNA (100-300 pg/embryos) and gRNA (7-30 pg/embryos) were microinjected into the one-to-four cell stage embryos. Between 500-600 embryos were injected per gene.

About 48 hours after microinjections, 30 randomly selected embryos were screened for mutations. DNA was extracted from these 30 embryos by treating with 100 μl of 50mM sodium hydroxide solution. The amplified PCR product was purified using QIAgen PCR purification kit and purified PCR product was screened for mutations with the T7 endonuclease assay. The T7 assay is comprised of two stages: a 20 minutes hybridization reaction followed by a 15 minute T7 endonuclease digestion reaction. The initial stage of the hybridization reaction denatures double strand of DNA and is conducted at 98°C. During the later stage of hybridization reaction, which is conducted over a ramp temperature from 98 to 55°C, complementary strands anneal with one

another. Hybridization reactions were conducted by using the Master Cycler Gradient thermal cycler (Eppendorf 5331) condition shown in tables 9a and 9b. The hybridization mixture was then digested by T7 Endonuclease at 37°C for 15 minutes. T7 endonuclease is known to cleave double-stranded DNA at mismatched bases. After 15 minutes of incubation, the digestion reaction mixture was stopped by adding 1μl of 0.25M EDTA. The sample was immediately electrophoresed on a 1% agarose gel. If the bands on the gel showed any sign of mutation, then we proceeded with cloning and sequencing to verify the mutation. For cloning, PCR product of the sample was ligated to pGEM-T vector by using the reagents shown in Table 5. Ligated DNA samples were transformed and screening for inserts using the same protocol described under the Methods section "TALENs-based genome editing mutagenesis."

Screening F0, F1, F2, and F3 Generations for *scn5Laa* and *ab* mutations

After bulk screening, the remaining embryos were raised and screened for specific mutations in *scn5Laa* and *ab* genes. When these embryos (F0 generation) reached sexual maturity, each individual injected fish-was mated with wild-type (WT) fish in order to generate F1 generation embryos. After 48hpf, about 30 F1 embryos from each injected F0 fish were screened for germ-line mutation by following the same procedure as above. If these embryos carried germ-line mutations from a specific F0 individual, then the rest of the F1 embryos from a particular F0 mutant were raised to adulthood for individual screening after reaching adulthood.

Once embryos from the F1 generation reached adulthood, each fish was screened for heterozygous mutation using the mutation screening assay described in Methods. Briefly about 20 mg of fin tissue was removed from the caudal fin by clipping it

off with a pair of fine scissors after anaesthetizing the fish with MS-222 (100 μg/ml for 1-2 minutes). The fin clip tissue was immersed in 50μl of 50mM sodium hydroxide solution to dissolve the tissue and extract DNA. The screening procedure for the F1 generation fish was exactly the same as above bulk screening procedure of the embryos. When at least one heterozygous mutation-bearing male and a female were identified through DNA sequence verification, were mated with each other to produce F2 generation embryos. Based on Mendelian principles of inheritance, 1/4th of these embryos were expected to be homozygous mutants in which both alleles were knocked out for either *scn5Laa* or *scn5Lab*. Once F2 generation embryos reached adulthood, individual fish were screened as described in methods to identify homozygous mutants. After homozygous mutants were verified via sequencing, a male and a female mutant were mated with each other to produce a fully homozygous F3 generation. All the embryos in the F3 generation of both *scn5Laa* and *scn5Lab* mutants were homozygous for the mutant alleles. Phenotypes of F3 generation embryos were observed and compared with wild-type embryos using stereomicroscope at 10 and 20X magnification. F3 generation and WT embryos were closely monitored under microscope starting 24 hpf for potential phenotypes such as gross pericardial edema, yolk-sac edema, reduced heart rate, and progressive thinning of the heart. If these phenotypes were evident in mutant embryos compared to WT embryos, mutant embryos were screened using sequencing for homo allelic mutation. If the F3 generation embryos did not show any defective cardiac phenotypes, random 20 embryos were screen to verify the homo allelic mutation in the expected region.

Additional Microinjections to Identify the Nature of Putative *scn5Laa* Mutants

Due to certain unexpected results of *scn5Laa* knocked out fish, additional microinjections were conducted to test a hypothesis that *scn5Laa* might be expressed as a dominant negative gene, with the potential to induce heart defects and lethality in F0 embryos and larval fish. Three different trials of microinjections were conducted in which between 300-400 embryos were microinjected with either *scn5Laa* gRNA or a control gRNA. For the control group, gRNA other than *scn5Laa* gRNA were used to control for lethality or gross morphological defects unrelated to *scn5Laa* or *ab* gRNA. For both gRNAs and Cas9, the same microinjection conditions-as described in Methods were used. Death rates and phenotypes of the F0 microinjected embryos from both groups were observed and compared.

Physiological and Developmental Characterization of *scn5Laa* and *ab* Knockout Mutants

Since zebrafish embryos and early stage larvae are optically clear, *scn5Laa* and *scn5Lab* knockout lines (heterozygous and homozygous mutants) were compared to wild-type controls by measuring their heartbeat rates at selected times during development. Both mutant and wild-type zebrafish were spawned around 9:00 am and the embryos were harvested anytime up until 1:00 pm. After 24 hpf (when the heart is first visible under a microscope), 3-5 embryos from control and mutation-bearing groups were dechorionated and embedded in 1% low melting point agarose prepared in stock zebrafish water on a microscopic slide. The embryos and larvae were observed under the stereomicroscope at 10 and 20X magnification at timed intervals post-spawning to determine if stereotypical heart developmental defects like gross pericardial edema,

reduced heart rate and progressive thinning of the heart were evident. Embryo and larval heart beat rate was measured by manually counting heart beats for 1 minute time intervals at three consecutive periods at each time point for each embryo. Heart beats of both control and mutant embryos were counted every two hours from 24 to 30 hpf. Heart beat rates were measured again for embryos that were 48 hpf for a period from 48 hpf to 54 hpf using the same procedure described above. These experiments were repeated three times from independently spawned embryos. We counted heartbeats of heterozygous and homozygous mutation-bearing embryos and compared them to each other and WT embryos. Statistical t-tests were conducted to determine whether there was a significant difference in the heartbeat rates of control group compared to mutants at each sample time. *Scn5Laa* homozygous knockouts were compared statistically and physiologically to *scn5Laa* heterozygous knockouts, *scn5Lab* homozygous knockouts and WT embryos. Similarly, *scn5Lab* homozygous knockouts were compared statistically and physiologically to *scn5Lab* heterozygous knockouts and WT embryos.

Vector	Volume (μl)
10X Tango Buffer	2.0
NheI	0.8
HindIII	0.8
pA (plasmid DNA)	16.4
Total	20.0

Insert	Volume (μl)
10X Tango Buffer	2.0
SpeI	0.8
HindIII	0.8
pT (plasmid DNA)	16.4
Total	20.0

Table 1: Reagents used for DNA restriction endonuclease digestion of vector and insert for RVD construction of TALENs

Ligation	Volume (μl)
5X T4 DNA Ligase buffer	2.0
Vector	1.0
Insert	6.9
T4 DNA Ligase	0.1
Total	10.0

Table 2: Reagents used for DNA ligation of vector and insert for RVD construction of TALENs

Reagents	Volume (μl)
Water (SDW)	6.55
5X Go Taq Buffer	2.0
$Mgcl_2$	1.0
dNTPs	0.2
Fw primer	0.1
Rv primer	0.1
DNA Taq Polymerase	0.05
DNA	1 transformed colony
Total	10.0

Table 3: Reagents used for PCR clone check to verify ligation of insert to vector

scn5Laa	Volume (μl)
1X Buffer O	4.0
PstI	3.2
Amplified PCR Product	32.8
Total	40.0

scn5Lab	Volume (μl)
1X Buffer B	4.0
ApaI	3.2
Amplified PCR Product	32.8
Total	40.0

Table 4: Reagents used to check the presence of indel mutation in the spacer region between TALENs target sites

The buffer and enzymes were ordered from Thermo Scientific.

Ligation Mixture	Volume (μl)
2X Rapid Ligation buffer	2.5
pGEM®-T or pGEM®-T Easy Vector (50 ng)	0.5
Gel purified PCR Product	1.5
T4 DNA Ligase	0.5
Total	5.0

Table 5: Reagents used for T-vector cloning ligation
The reagents were obtained from Promega.

Incubation	Time (minutes)
Incubate at 37°C	30
Incubate at 95°C	5
Ramping down to 25 °C at 5°C/min (0.08 °C/sec)	

Table 6a: Phosphorylation and annealing conditions for oligonucleotides in PCR

Reagents	Volume (μl)
sgRNA Oligos Forward (100 μm)	1.0
sgRNA Oligos Reverse (100 μm)	1.0
10X T4 Polynucleotide Kinase (PNK) buffer	1.0
T4 PNK	1.0
Water	6.0
Total	10.0

Table 6b: Reagents added to anneal and phosphorylate oligonucleotides

Reagents	Volume (μl)
pT7-gRNA Plasmid (~202 ng/μl)	16.4
10X OPTIZYME Buffer 3	2.0
BglII	0.8
SalI	0.8
Total	20.0

Table 7a: Reagents added for first digestion reaction to linearize pT7-gRNA vector

Reagents	Volume (μl)
Purified pT7-gRNA Plasmid	30.0
10X OPTIZYME Buffer 4	4.0
DTT (20mM)	2.0
EpsI (BsmBI)	3.2
Water	0.8
Total	40.0

Table 7b: Reagents added for second digestion reaction to linearize purified pT7-gRNA vector

Reagents	Volume (μl)
2X Rapid Ligation Buffer	2.5
Linearized pT7-gRNA Vector	1.0
Diluted Oligos (1:200)	1.0
T4 DNA Ligase	0.5
Total	5.0

Table 8: Ligation of oligonucleotides to pT7-gRNA Vector

Reagents	Volume (μl)
NEB Buffer 2	1.0
Purified PCR product	8.5

Table 9a: Conditions for T7 Endonuclease Assay

Incubation	Time (minutes)
Incubate at 95°C	5
Ramp Down to 85°C at -2°C/s	
Ramp down to 25 °C at -1°C/s	
Final Hold at 4°C	

Table 9b: Condition for Hybridization Reaction in Thermal cycler

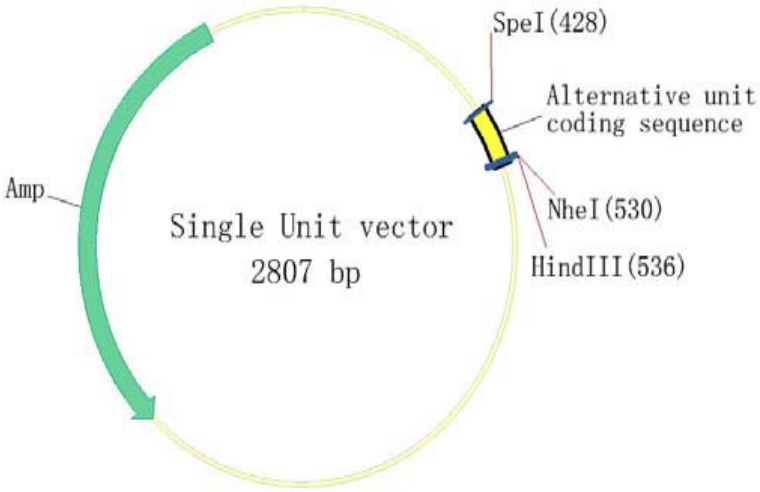

Figure 6: The representative plasmid structure of the single unit vectors for TALENs-TALE synthesis (Huang et al. 2011)

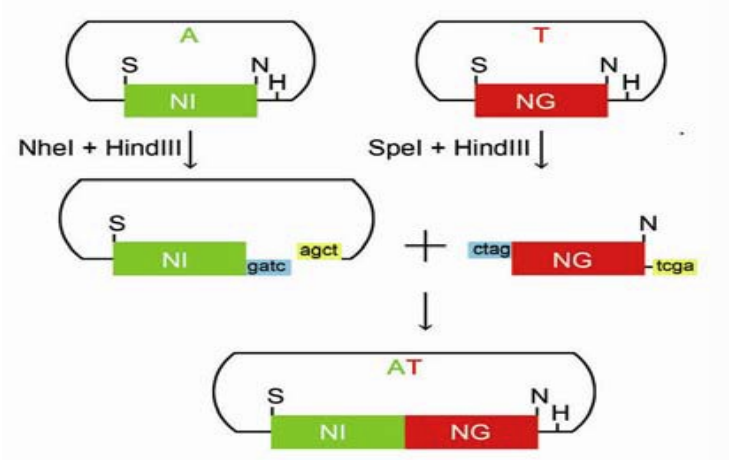

Figure 7: Schematic Diagram showing steps in the construction of vector pAT recognizing nucleotide sequences of 5'-AT-3' (Huang et al. 2011)

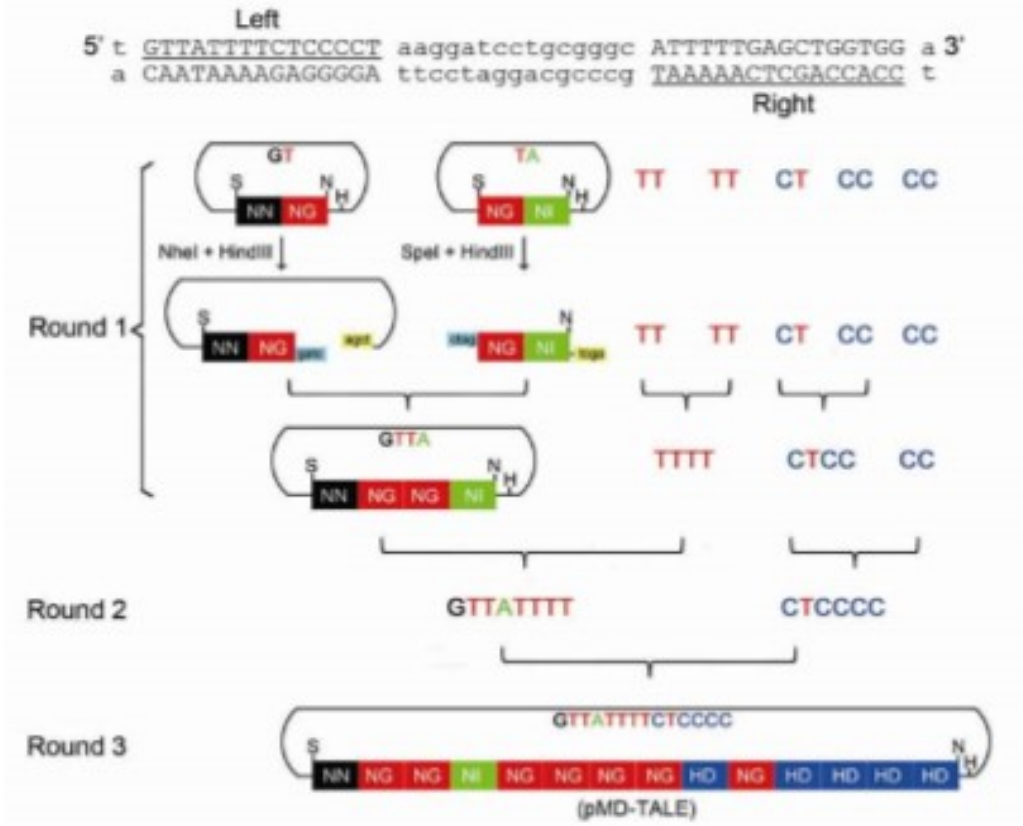

Figure 8: Schematic Diagram showing the construction of pMD-TALE vector with multiple TALE repeats (Huang et al. 2011) The assembly of the TALE repeats for the left *TALE binding site* of *tnikb* gen

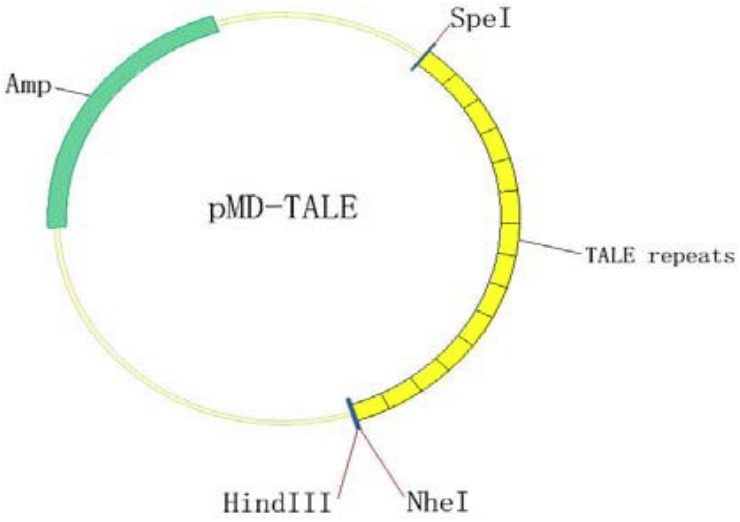

Figure 9: The representative plasmid structure of pMD-TALE vectors (Huang et al. 2011)

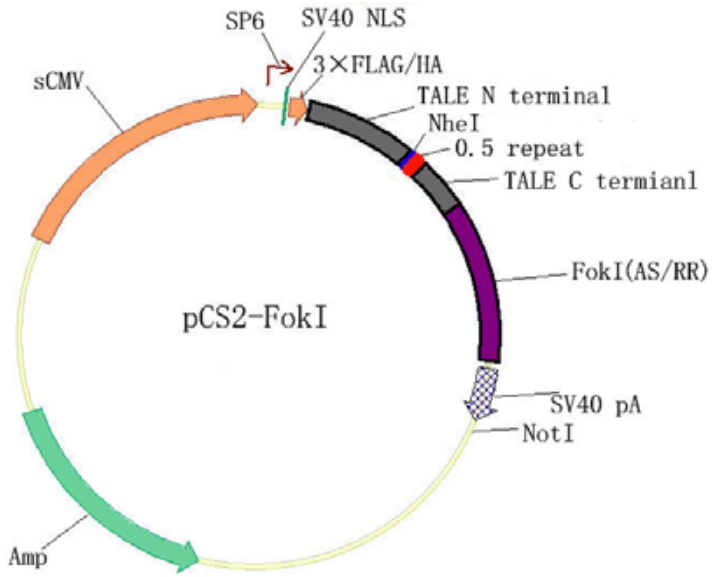

Figure 10: The representative plasmid structure of pCS2-FokI vectors (Huang et al. 2011)

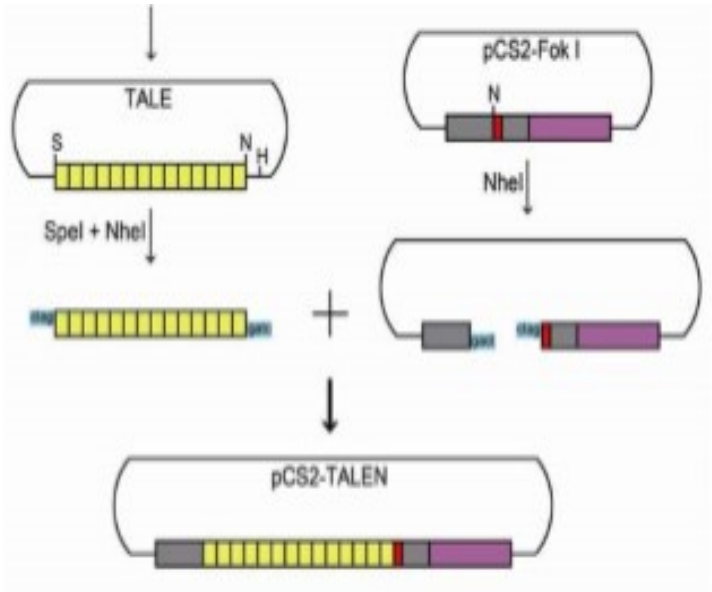

Figure 11: Schematic diagram for the construction of pCS2-TALEN vectors (Huang et al. 2011)

CHAPTER 3: RESULTS

TALENs authentication

The *scn5Laa* and *ab* gene-targeting TALENs were authenticated by a combination of restriction endonuclease mapping and direct DNA sequencing. After assembly and cloning of 16 unit TALENs into PEAS-TALENs and PERR TALENs (forward and reverse TALE binding sites, respectively) for both *scn5Laa* and *scn5Lab,* the plasmids (PEAS-TALENs and PERR TALENs) were double digested with *Nhe*I and *Kpn*I. Based on the DNA sequence of PEAS-TALENs and PERR TALENs plasmids, the *Kpn*I restriction site is 441bp upstream of *Nhe*I restriction site on pCS2-FokI vector (Huang et al. 2011). The total size of the vector backbone pCS2-PERR was 5458bp. The total size of 16 unit assembly for TALENs target site was 1632bp. If the insert is in the forward orientation, the clone is predicted to generate fragments of 2073bp (441bp + Insert size of 1632bp) and 5017bp (vector size – 441bp) after double digestion with *Nhe*I and *Kpn*I (Figure 12-lane 11). Figure 12 shows a gel image of 16 unit insert ligation to PERR-TALENs plasmid for the *scn5Laa* reverse site. There is a possibility of this insert to ligate into the reverse direction to the vector. If the insert is in the reverse direction, the fragments are predicted to be 441 and 7090 (Figure 12-lane 13). If the vector self-ligated without insert in it, the prediction is for fragments of 5017 bp and 441 bp (Figure 12-lanes 2, 10, 12). Since 441 bp is significantly smaller than other bands, they were predicted to travel faster on the gel and are not readily visible. Lanes 3, 4, 5, and 9 of Figure 12 represents clones containing just inserts that did not successfully ligate to the pCS-PERR vector. As shown in Figure 12, only lane 11 showed bands at 5017bp and 2073bp, which is indicative of an insert in the correct (forward) orientation.

Based on this information the PERR-TALENs plasmid insert from the *E.coli* clone representing lane 11 was sequenced using the SP6 primer to verify orientation and sequence of the insert. Sequence analysis verified that the clone referred to as *scn5Laa* PERR-TALENs #11 contained an insert in the forward direction representing a 16 unit TALENs assembly designed to target nucleotides GTCTCAGGATCCCCATG.

The same approach was used to verify the orientation and sequence of inserts for *scn5Lab* PEAS-TALENs and PERR-TALENs plasmids. Figure 13 shows a gel image of 16 unit insert ligation to PEAS-TALENs plasmid and 18 unit insert ligation to PERR-TALENs plasmid for the *scn5Lab* forward and reverse TALENs target site, respectively. For *scn5Lab*, the 16 unit assembly for the forward TALENs binding site (PEAS-TALENs) had an insert of 1632 bp; whereas, the 18 units assembly for reverse TALENs binding site (PERR-TALENs) had an insert of 1836 bp. Lanes 1-11, 13, 14, and 19 in Figure 13 represent bands from the double digestion with *Nhe*I and *Kpn*I of PEAS-TALENs plasmid of *scn5Lab*. Lanes 12, 15-18, 20-28 in Figure 13 represent bands from the double digestion with *Nhe*I and *Kpn*I of PERR-TALENs plasmid of *scn5Lab*. The clones with inserts in forward orientation for PEAS-TALENs site produced bands at 5017 bp and 2073 bp (Figure 13-lanes 13, 14, 19). The clones with inserts in reverse orientation produced bands at 7090 bp and 441 bp (Figure 13-lanes 2, 3). Self-ligated vector produced bands at 5017 bp and 441 bp (Figure 13-lanes 9, 11). Lanes 1, 6, and 10 of Figure 13 represent undigested vector producing band at 5458 bp. Since PERR-TALENs plasmid is composed of 18 units, insert in the forward direction produced bands at 2277 bp and 5017 bp (Figure 13-lanes 12, 20, 23, 26). Insert in the reverse direction produced bands at 7294 bp and 441 bp (Figure 13-lanes 16, 18, 24, 25, 27,

28). Self-ligated vector produced bands at 5458 bp and 441 bp (Figure 13-lanes 15, 17). Clone numbers 13, 14 (PEAS-TALENs site) and 20, 23 (PERR-TALENs site) were verified for the forward insert orientation via sequencing using the SP6 primer.

Identification of TALENs-induced mutations in zebrafish

To confirm the general capability of *scn5Laa* and *ab*-directed TALENs to induce mutations at their respective target sites in zebrafish embryos after microinjection, about 30 embryos microinjected with TALENs directed toward *scn5Laa* or ab genes were screened using the bulk screening approach described in Methods. Results from digestions of PCR amplification products obtained from DNA extracted from pooled TALENs microinjected embryos are shown in Figures 14, 15, 31, 32. Figures 14 and 15 show gel image and sequencing data from bulk screening of the embryos injected with TALENs molecules targeting forward and reverse sites, CAGTGTCTTCGCTCTGA and GTCTCAGGATCCCCATG, respectively in exon 7 of *scn5Laa*. Lane 4 of Figure 14 shows two bands compared to other bands on the gel. The top band in lane 4 (indicated by an arrow) represents product expected if the *PstI* restriction site was inactivated by mutation in the spacer region (TCGGTCTGCAGCTCTT). The top band representing undigested mixture was 201 bp long. The second band in lane 4 represents wild-type sequence. The digested products are expected to produce two bands at 95 bp and 106 bp. Since these two bands are approximately the same in size, they overlap on the gel showing one broad and relatively intensely staining band instead of two separate bands. Bands in lanes one and two of Figure 14 show control samples producing digested products. Figure 31 shows a gel image from bulk screening of *scn5Lab* TALENs-targeted embryos in exon 5. *Scn5Lab* TALENs target site for the forward and the

reverse sites were CCTGGCGCGGGGTTTCT and TCCAGGGGTCCCTCAGAAA, respectively. Lane 4 of Figure 31 shows bands that were 361 bp, 310 bp and 104 bp long. The 361 bp fragment represents the product expected if the *Apa*I restriction site was inactivated by mutation in the spacer region (GCATCGGGCCCTTCACA), while the two fragments at 310 bp and 104 bp in length represents the digestion products of PCR products derived from DNA in which the restriction site was unaltered. Based on these results, it was concluded that the TALENs were effective in inducing mutations in the spacer region (GCATCGGGCCCTTCACA). However, the exact percentage of embryos in which mutations were induced cannot be accurately determined using this bulk screening approach. In Figures 14 and 31, the arrow points to an undigested product with an additional band at 201 bp and 361 bp, respectively compared to control wild-type (WT). Additional bands representing mutations in both *scn5Laa* and *scn5Lab* were cloned and sequenced using the T7 primer. Between 5-8 clones were selected for *scn5Laa* and *scn5Lab* to sequence. Figures 15 and 32 show the sequencing results for clones derived from DNA fragments purified PCR products for either *scn5Laa* or *scn5Lab* genes, respectively. In Figure 15, clone numbers 1 and 7 show deletions of -3bp and -8bp, respectively, relative to the wild-type sequence. The 3 bp deletion in clone #1 causes an in-frame mutation leading to one missing amino acid. However, sequencing data from clone #2 shows an 8 bp deletion that cause a frameshift mutation in the coding region. Overall, the data shows that out of 30 embryos screened, one of them possess in-frame mutation while the other one is carrying frameshift mutations. This data suggests that there is a 50% chance of these embryos showing frame-shift mutations once they reach adulthood. Only 60 fish survived and reached adulthood

from this batch. Out of these 60, none of them showed any mutation at the targeted sequence. Figure 32 shows various mutations for *scn5Lab* compared to WT including +4bp insertion, -13bp deletion, and a single nucleotide polymorphism (SNP). The data shows that most of the embryos injected with TALENs *scn5Lab* mRNA have frameshift mutation.

After the F0 embryos reached sexual maturity, each individual fish was screened for germline cell transmission of mutations by mating with WT and examining their offspring for the mutant allele in a heterozygous condition. F1 offspring were screened for mutations as early as 48hpf. In the case of *scn5Laa*-targeted fish only, no germline cell transmission of mutations was observed on gels after PCR amplification and digestion of DNA prepared from F1 offspring. We screened 60 individual adult fish and did not find any mutants. The digested product looked exactly like control wild-type product on the gel. By comparison, two *scn5Lab* F0 males showed germline transmission of their respective mutations after screening 75 individual fish. Embryos from these mutant males (#3-8 and 5-6) were screened using the same protocol as described in methods. Figures 34 and 36 clearly show the additional third band (designated by arrows) indicating the undigested product as a sign for mutation. This band was gel extracted and sequenced in order to verify the mutation. Figure 35 shows the changes in DNA sequence of the mutant #3-8 compared to WT. The sequencing result provides evidence for a 5 bp deletion compared to WT strand. Furthermore, Figure 35 shows that this frameshift leads to a frame-shift in the amino acid sequence compared to WT starting at amino acid 182. In the WT strand, the 182nd amino acid is glycine (G); whereas, in the mutant strand the frameshift changed the 182 amino acid to

leucine and all amino acids up to the stop codon at 203 were also altered. The normal length of the protein product for *scn5Lab* is 1954 amino acids. Figure 36 shows gel image for mutant #5-6. Figure 37 shows changes in the DNA sequences of mutant #5-6 compared to WT. In this case, there was a 15 bp deletion compared to WT strand which caused a five amino acid in-frame mutation. Furthermore, Figure 37 shows that amino acids 1-179 are exactly the same as WT. Due to in-frame mutation, amino acids 180-184 are missing in mutant #5-6 compared to WT protein; however, based on DNA sequence the remainder of mRNA and resultant amino acids (185-1954) could be translated.

When F1 generation offspring from mutant #3-8 reached adulthood, about 50 individual fish were screened and yielded 4 heterozygous TALENs-induced mutants. The gel image (Figure 34) and sequencing results of these 4 fish were exactly the same as their male parent mutant #3-8. Their hetero allelic mutation had 5 bp deletion compared to WT strand which caused a frameshift mutation as shown in Figure 35. After sequence verification of the mutation, four F1 heterozygous mutants were mated with each other to produce F2 generation offspring. According to Mendelian genetics, 25% of the F2 generation is expected to have homozygous null mutations for *scn5Lab*. Physiological examination of the F2 generation embryos revealed that 7% of these embryos showed abnormal cardiac phenotypes 6dpf as shown in Figure 40. These embryos showed significant pericardial edema, yolk-sac edema, and died prematurely. These embryos were sequenced to determine if they carried the F1 parent frame-shift mutation. The embryos that died prematurely after showing abnormal cardiac and yolk-sac edema showed homozygous null allele mutation. Surprisingly, when the remaining

embryos from this batch reached adulthood, we found additional homozygous null allele mutants that were able to develop normally. When we screened 14 of the remaining F2 generation fish once they reached adulthood, five of them showed homozygous null allele mutation. These fish had the exact same frame-shift mutation as the other embryos that showed cardiac and yolk-sad edema and ended up dying prematurely. Once F2 generation adult fish were sequence verified, we mated those with each other to produce F3 generation offspring. As expected, 100% of F3 generation offspring are homozygous null allele mutants for *scn5Lab*. Unfortunately, embryos from these F3 generation fish did not show us any abnormal developmentally defective phenotypes.

Identification and characterization of CRISPR-CAS9 Induced Mutants

Given the absence of TALENs-induced *scn5Laa*-induced mutations and the relatively low number of TALENs-induced *scn5Lab*-induced mutations, further genome editing experiments were conducted using the CRISPR-CAS9 genome editing system. Just like TALENs, the screening process was conducted in two stages, a bulk screening stage and a single animal screening stage. In the case of CRISPR-CAS9-induced mutations, the screening was not conducted by restriction endonuclease digestion of PCR product, instead -purified PCR products were screened using the mismatch cleavage activity of T7 endonuclease at the CRIPSR-CAS9 target sites. The CRISPR-CAS9 target site for *scn5Laa* was GGATTTCAGTGTCATCGTCATGG located in exon 5. Mutation resulting from CRISPR-CAS9 induction show up as 3 distinct bands on the gel. Figure 16 shows a gel image of bulk screening of 30 embryos at 48 hpf for *scn5Laa*. The first band shown in lane 2 of Figure 16 represents undigested product after T7 endonuclease digestion. Since T7 endonuclease cleaves at the mismatched

DNA base pair site, the potential bands after the cleavage are supposed to be 462 bp and 176 bp, respectively for *scn5Laa*. However, Lane 2 shows four bands after T7 assay. The first band is 638 bp long and corresponds in length to the expected undigested PCR product. We surmise the second band occurs because of a sequence polymorphism. We hypothesize that the second band represent a sequence polymorphism in wild-type zebrafish because a band around ~500bp is not expected from T7 endonuclease, and since our positive control in lane 3 also shows a band around 500 bp, it is believed that T7 endonuclease also cleaved an additional site resulting from the naturally occurring polymorphism. The third and fourth bands which are 462 bp and 176 bp in length are products expected from T7 endonuclease cleavage of the PCR product resulting from mutationally-induced mismatches between wild-type sequence and mutation-bearing sequences. Lane 3 shows bands for the positive control which has bands at the exact same sizes at lane 2. Lane 4 has a marker for undigested control of 638bp which is difficult to visualize in the gel image due to loading dye masking the DNA-containing band. Figure 17 shows sequencing data from the bulk screening procedure for verification of the mutation inducing activity of the *scn5Laa* targeting gRNA. 30 embryos were screened from 500-600 embryos that were microinjected. Clone #2 shows 5 bp deletion causing a frame-shift in the coding region that can result premature translation termination (Figure 17). Clone #5 shows 3 bp deletion causing an in-frame mutation compared to WT strand. Data from Figure 17 suggests that these embryos have a 50% chance of having either frame-shift or in-frame mutation. It was assumed that a similar proportion of the remaining microinjected

embryos would have mutations as well. However, only 8% of these embryos (1/13) showed frame-shift mutation once they reached adulthood.

Consequently, the remainder of the embryos were grown to the adult stage and screened for mutations in DNA obtained from fin-clips. Screening 50 individual fish revealed 13 potential F0 mutants (see Figures 18-30). The gel images show three distinct bands for each of the digested PCR amplification products, a property expected for sequences bearing mutations. However, DNA sequencing results shown in Figures 18-29 show that deletions present in fish #1, 4, 14, 15, 17, 32, 34, 42, 44, 49, 52, and 55 resulted in in-frame mutation. However, mutant number 7 (shown in Figure 30) had a two nucleotide frameshift which is predicted to prematurely terminate translation after amino acid 210 compared to the wild-type protein, which is 1932 amino acids long. Mutant #7 was crossed with wild-type to generate F1 heterozygotes. Of 30 adult F1 fish, 5 were determined to be heterozygote CRISPR-CAS9 induced mutation-bearing fish. These mutants were sequence verified to make sure they inherited the same mutation shown in Figure 30 from their mother. After sequence verification, these 5 mutants were mated with each other to produce F2 generation offspring. Again, 25% of these offspring are expected to be homozygous null allele mutants for *scn5Laa*. We did not observe any developmental defective phenotypes when these embryos from these crosses were growing. Once the embryos reached adulthood, we screened 37 fish and identified 7 homozygous mutants based on DNA sequence analysis of PCR amplified and cloned genomic DNA. These homozygous mutants were mated with each other after sequence verification to produce F3 homozygotes. 100% of F3 generation offspring were expected to be homozygous null mutants. Stereomicroscopic screening

of these F3 homozygous mutants did not reveal a higher portion of developmentally defective mutants than suitable wild-type controls.

To determine why *scn5Laa* embryos had a high percentage of in-frame mutants compared to frameshift mutants, we microinjected more WT embryos with *scn5Laa* gRNA and screening for embryonic lethality and induction of developmental defects. We conducted independent replicate microinjections trials each one week apart using wild-type zygotes prepared from different wild-type parents. These embryos scored beginning at 24hpf for developmental defects and lethality phenotype. Between 50hpf to 80hpf we saw the most developmental defective phenotypes including premature death of the embryos compared to control injected group. We consistently observed 25-35% death during embryonic development for *scn5Laa* gRNA injected embryos compared to 5-7% death in the control group. Moreover, 3-10% of the embryos injected with *scn5Laa* gRNA showed developmentally defective phenotypes in each of the three trials but none in the control group. Figure 41 shows developmental defects caused by injection of *scn5Laa* gRNA. These defects include cardiac edema, yolk sad edema, curvature of spine, and premature embryonic death. Extracted DNA from these embryos were cloned in order to determine the genotype of these embryos. Mutations were not detected in any of the developmentally defective embryos.

Heartbeat Rate and Developmental Phenotype Characterization of TALENs and CRISPR-CAS9-Incduced *scn5Laa* and *ab* Mutants

Statistical comparison of the differences in heartbeat rate of heterozygous and homozygous knockout embryos for either *scn5Laa* or *scn5Lab* did not show any difference between the heart rate compared to each other or to the WT embryos at any

time periods for first three days of development (Table 10), which is the critical time period for observing expected heart defects. Figure 42 shows the comparison of heartbeat between *scn5Laa* heterozygous and homozygous embryos with *scn5Lab* heterozygous and homozygous embryos and WT embryos. The bar graphs in Figure 42 shows that the heart rate of these embryos are very similar to each other at any given time period. Moreover, knockouts did not show any significant gross development phenotypic differences and were able to grow normally through the larval stage of development. We were successfully able to sequence 20 embryos from each batch to verify homo allelic mutation. These data suggest that knockout of either *scn5Laa* or *scn5Lab* individually had no effect on the developmental or physiological characteristic of the heart.

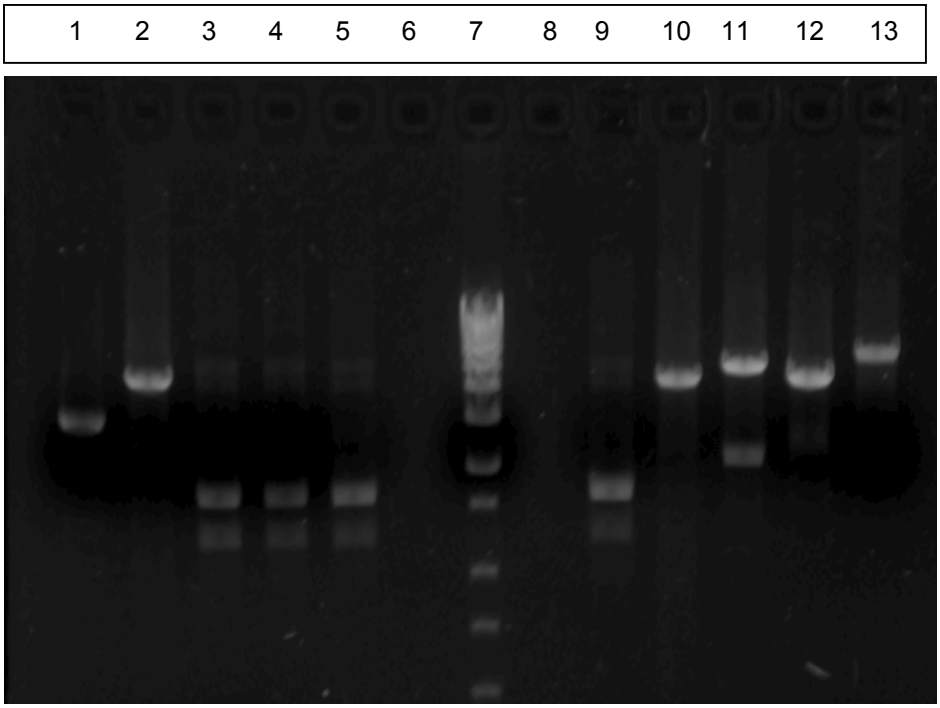

Figure 12: Sixteen unit TALEN assembly for *scn5Laa* gene reverse target site
Lanes 1-5 and 9-13 represent fragment patterns from DNA obtained from *E. coli* clones after double digestion (with *Nhe*I and *Kpn*I) and electrophoresis of the plasmid PERR-

TALENs for *scn5Laa*. Lane 7 is the 1 kb molecular length standard (Life Technologies). Lane 11 represent insert in the forward direction by producing bands at 5017 bp and 2073 bp. Lanes 13 represent insert in the reverse direction by producing bands at 7090 bp and 441 bp. Lanes 2, 10, 12 represent vector self-ligating by producing bands at 5017 bp and 441 bp. Since bands at 441 bp were predicted to travel faster on the gel, they are not readily visible. Lanes 3-5 and 9 represent clones containing only inserts.

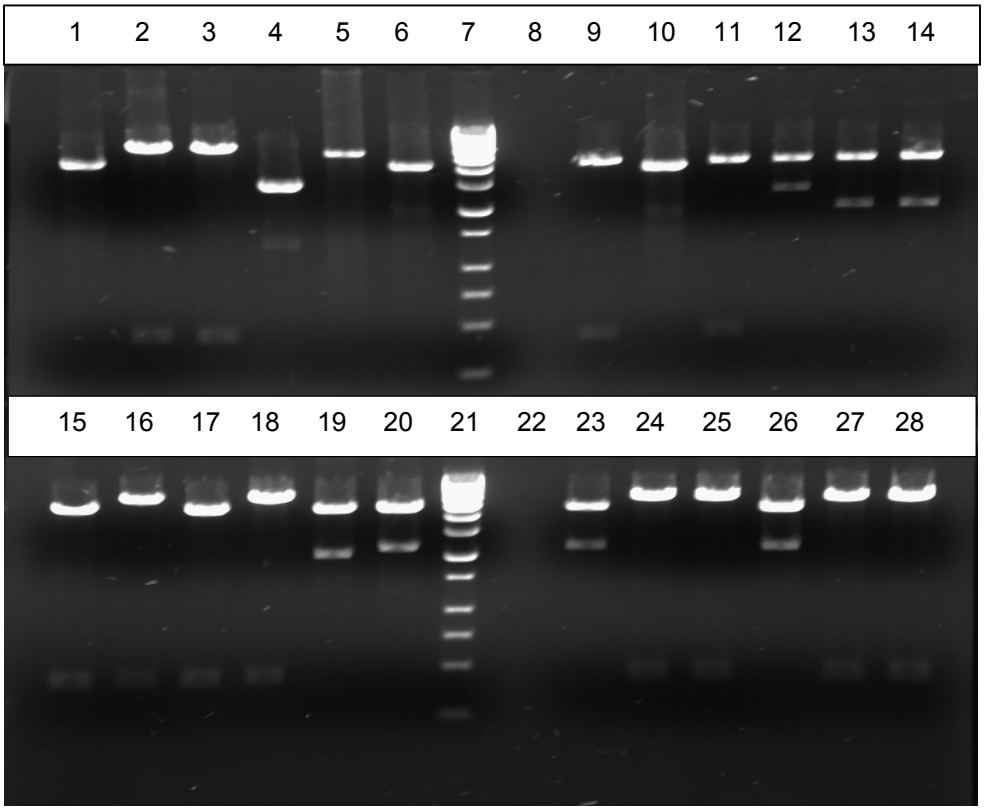

Figure 13: Sixteen-eighteen unit TALEN assembly for *scn5Lab* forward and reverse target sites. Lanes 1-6, 9-11, 13, 14, and 19 represent fragment patterns from DNA obtained from *E. coli* clones after double digestion (with *Nhe*I and *Kpn*I) and electrophoresis of the plasmid PEAS-TALENs for *scn5Lab;* whereas, lanes 12, 15-18, 20, 23-28 represents fragment patterns of plasmid PERR-TALENs for *scn5Lab*. Lanes 12, 14, 19 represent clones containing insert in the forward direction for PEAS-TALENs producing bands at 5017 bp and 2073 bp. Clones in lanes 2 and 3 represent insert in the reverse direction producing bands at 7090 bp and 441 bp. Clones in lanes 9 and 11 represent self-ligating vector producing bands at 5458 bp. Lanes 1, 6, and 10 represent undigested sample producing a single band at 5458 bp. Lanes 12, 20, 23, and 26 represent insert in the forward direction for plasmid PERR-TALENs representing bands at 5017 bp and 2277 bp. Lanes 16, 18, 24, 25, 27, 28 represent insert in the reverse direction producing bands at 7294 bp and 441 bp. Lanes 15, 17 shows bands for self-ligating vector at 5458 bp and 441 bp.

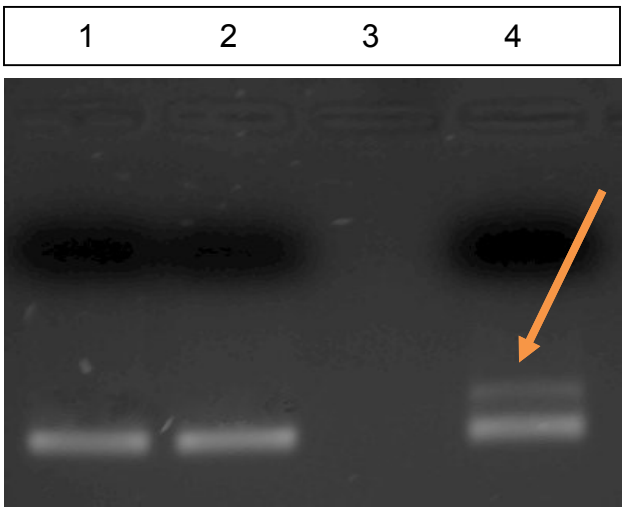

Figure 14: Gel Image to show *scn5Laa* F0 Bulk Screening mutation. Lane 1 represents F0 generation of *scn5Laa* PCR product digested with *Pst*I with no indication of indel mutations producing overlapping bands at 106 bp and 95 bp. Lane 2 represents WT digested sample producing overlapping bands at 106 bp and 95 bp. Lane 4 shows F0 generation *scn5Laa* PCR product digested with *Pst*I producing two bands indicated indel mutation. The top band is 201 bp long indicated undigested product due to the presence of indel mutation. The bottom band is an overlap of two bands (at 106 bp and 95bp) showing the digested mixture indicating presence of no indel mutations in some of the 30 embryos that were screened.

	CAGTGTCTTCGCTCTGATCGGTCTGCAGCTCTTCATGGGGATCCTGAGAC	(WT)
(1)	CAGTGTCTTCGCTCTGATCGGTCTGCA------CTTCATGGGGATCCTGAGAC	(-3)
(7)	CAGTGTCTTCGCTCTGATCGGTCT----------TCATGGGGATCCTGAGAC	(-8)

Figure 15: Sequencing results of *scn5Laa* Bulk Screening
The highlighted portion refers to *scn5Laa* TALENs forward and reverse binding sites targeted from plasmid *scn5Laa* PEAS-TALENs and PERR-TALENs, respectively. Clone #1 shows 3 bp deletion compared to WT strand; whereas, clone # 7 represents 8 bp deletion compared to WT strand in the spacer region of TALENs targeted site.

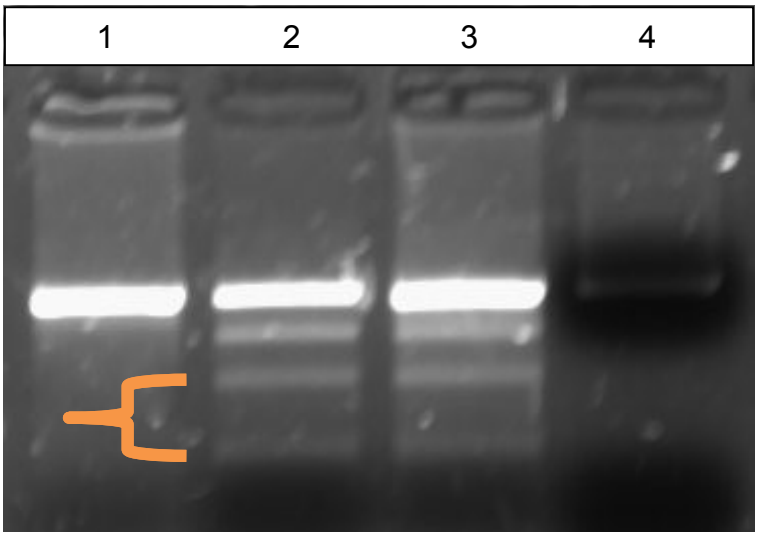

Figure 16: Bulk screening F0 CRISPR-CAS9 injected embryos for *scn5Laa*
Lane 1 represents wild-type PCR amplification product after T7 endonuclease digestion showing just a single band at 638 bp. Lane 2 shows PCR amplification product from bulk embryo clutch treated with CRISPR-CAS9 RNA after T7 endonuclease digestion producing four bands. First band is 638 bp long representing undigested products. Second band is for polymorphism since band around 500 bp is not expected. Last two bands represent the presence of indel mutation. Cleavage site of CRIPSR RNA is predicted to produce bands at 462 bp and 176 bp. Lane 3 shows *scn5Laa* Positive control obtained from a sample known to produce bands corresponding mutation. Lane 4 represents undigested PCR amplified product from bulk embryos to run as a marker for 638 bp.

```
    TGGAACTGGCTGGATTTCAGTGTCATCGTGGCGTGAGT (WT)
(2) TGGAACTGGCTGGATTTCAGTGT-----TGGCGTGAGT (-5)
(5) TGGAACTGGCTGGATTTCAGTGTCA---TGGCGTGAGT (-3)
```

Figure 17: Sequencing results of *scn5Laa* Bulk Screening
Highlighted portion refers to 23 bp CRISPR-CAS9 target site for *scn5Laa.* Clone # 2 shows 5 bp deletion compared to WT strand; whereas, clone # 5 represents a 3 bp deletion compared to the WT strand.

Scn5Laa F0 Mutant #14-4

GGATTTCAGTGTCATCGTCATGG (wt)

GGATTTCAGTG------TCATGG (-6)

1930 aa. Missing Isoleucine and valine (199-200 aminoacids)

MATMLLPAGPDGLRPFTRESLAAIEQRISEERARNTKDYKADPGDVEEPKPRADLEVGKV
LPRIFGEIPAGLVGVPLEDIDPFYFRNQKTFIVLNKGKAIFRFSATSALYIFSPFHCIRR
ISIRILVHSLFSLFIMCTILTNCCFMAMSDPPLWTKYLEYTFTGIYTFESLIKILARGFC
TECFTFLRDPWNWLDFSV–MAYVTEFVDLGNV. . . (+1719)

WT Scn5Laa, 1932 aa

MATMLLPAGPDGLRPFTRESLAAIEQRISEERARNTKDYKADPGDVEEPKPRADLEVGKV
LPRIFGEIPAGLVGVPLEDIDPFYFRNQKTFIVLNKGKAIFRFSATSALYIFSPFHCIRR
ISIRILVHSLFSLFIMCTILTNCCFMAMSDPPLWTKYLEYTFTGIYTFESLIKILARGFC
TECFTFLRDPWNWLDFSVIVMAYVTEFVDLGNV. . . (+1719)

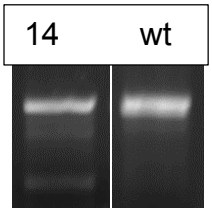

Figure 18: *scn5Laa* gene F0 Mutant #14, in-frame mutation. Mutant # 14-4 shows 6 bp deletion (in-frame mutation) compared to WT strand. The highlighted portion refers to this protein missing isoleucine and valine compared to WT production. The gel image shows three bands, at 638 bp, 462 bp, and 176 bp compared to WT strand producing only one band at 638 bp representing undigested mixture.

Scn5Laa F0 Mutant#15

GGATTTCAGTGTCATCGTCATGG (wt)

GGATTTCAGTGTCA---TCATGG (-3)

1931 aa. Missing valine (200th aminoacid)

MATMLLPAGPDGLRPFTRESLAAIEQRISEERARNTKDYKADPGDVEEPKPRADLEVGKV
LPRIFGEIPAGLVGVPLEDIDPFYFRNQKTFIVLNKGKAIFRFSATSALYIFSPFHCIRR
ISIRILVHSLFSLFIMCTILTNCCFMAMSDPPLWTKYLEYTFTGIYTFESLIKILARGFC
TECFTFLRDPWNWLDFSVI-MAYVTEFVDLGNV. . . (+1719)

WT Scn5Laa, 1932 aa

MATMLLPAGPDGLRPFTRESLAAIEQRISEERARNTKDYKADPGDVEEPKPRADLEVGKV
LPRIFGEIPAGLVGVPLEDIDPFYFRNQKTFIVLNKGKAIFRFSATSALYIFSPFHCIRR
ISIRILVHSLFSLFIMCTILTNCCFMAMSDPPLWTKYLEYTFTGIYTFESLIKILARGFC
TECFTFLRDPWNWLDFSVIVMAYVTEFVDLGNV. . . (+1719)

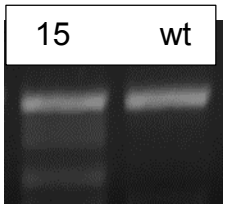

Figure 19: *scn5Laa* gene F0 Mutant#15, in-frame mutation. Mutant # 15 shows 3 bp deletion (in-frame mutation) compared to WT strand. The highlighted portion refers to this protein missing valine compared to WT protein production. The gel image shows three bands, at 638 bp, 462 bp, and 176 bp compared to WT strand producing only one band at 638 bp representing undigested mixture.

Scn5Laa F0 Mutant#17

GGATTTCAGTGTCATCGTCATGG (wt)

GGATTTCAGTGTCATCG---TGG (-3)

1931 aa. Missing Methionine (201st aminoacid)

MATMLLPAGPDGLRPFTRESLAAIEQRISEERARNTKDYKADPGDVEEPKPRADLEVGKV
LPRIFGEIPAGLVGVPLEDIDPFYFRNQKTFIVLNKGKAIFRFSATSALYIFSPFHCIRR
ISIRILVHSLFSLFIMCTILTNCCFMAMSDPPLWTKYLEYTFTGIYTFESLIKILARGFC
TECFTFLRDPWNWLDFSVIV-AYVTEFVDLGNV. . . (+1719)

WT Scn5Laa, 1932 aa

MATMLLPAGPDGLRPFTRESLAAIEQRISEERARNTKDYKADPGDVEEPKPRADLEVGKV
LPRIFGEIPAGLVGVPLEDIDPFYFRNQKTFIVLNKGKAIFRFSATSALYIFSPFHCIRR
ISIRILVHSLFSLFIMCTILTNCCFMAMSDPPLWTKYLEYTFTGIYTFESLIKILARGFC
TECFTFLRDPWNWLDFSVIVMAYVTEFVDLGNV. . . (+1719)

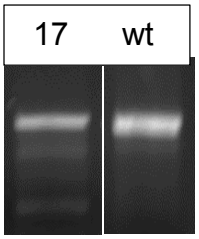

Figure 20: *scn5Laa* gene F0 Mutant#17, in-frame mutation. Mutant # 17 shows 3 bp deletion (in-frame mutation) compared to WT strand. The highlighted portion refers to this protein missing methionine compared to WT protein production. The gel image shows three bands, at 638 bp, 462 bp, and 176 bp compared to WT strand producing only one band at 638 bp representing undigested mixture.

Scn5Laa F0 Mutant #4

GGATTTCAGTGTCATCGTCATGG (wt)

GGATTTCAGTG---------TGG (-9)

Aminoacid 1932aa (1-198 aa same as WT, 197-199 missing)
MATMLLPAGPDGLRPFTRESLAAIEQRISEERARNTKDYKADPGDVEEPKPRADLEVGKV
LPRIFGEIPAGLVGVPLEDIDPFYFRNQKTFIVLNKGKAIFRFSATSALYIFSPFHCIRR
ISIRILVHSLFSLFIMCTILTNCCFMAMSDPPLWTKYLEYTFTGIYTFESLIKILARGFC
TECFTFLRDPWNWLDFS---MAYVTEFVDLGNV. . . (+1719)
WT Scn5Laa, 1932aa

MATMLLPAGPDGLRPFTRESLAAIEQRISEERARNTKDYKADPGDVEEPKPRADLEVGKV
LPRIFGEIPAGLVGVPLEDIDPFYFRNQKTFIVLNKGKAIFRFSATSALYIFSPFHCIRR
ISIRILVHSLFSLFIMCTILTNCCFMAMSDPPLWTKYLEYTFTGIYTFESLIKILARGFC
TECFTFLRDPWNWLDFSVIVMAYVTEFVDLGNV. . . (+1719)

Figure 21: *scn5Laa* gene F0 Mutant#4, in-frame mutation. Mutant # 4 shows 9 bp deletion (in-frame mutation) compared to WT strand. The mutant is missing valine, isoleucine, and valine from its protein product compared to WT protein production.

Scn5Laa F0 Mutant #1

GGATTTCAGTGTCATCGTCATGG (WT)

GGATTTCAGTGTCA------TGG (−6)

Aminoacid 1932aa (1-198 aa same as WT, 197-198 missing)

MATMLLPAGPDGLRPFTRESLAAIEQRISEERARNTKDYKADPGDVEEPKPRADLEVGKV
LPRIFGEIPAGLVGVPLEDIDPFYFRNQKTFIVLNKGKAIFRFSATSALYIFSPFHCIRR
ISIRILVHSLFSLFIMCTILTNCCFMAMSDPPLWTKYLEYTFTGIYTFESLIKILARGFC
TECFTFLRDPWNWLDFSV--MAYVTEFVDLGNV. . . (+1719)

WT Scn5Laa, 1932aa

MATMLLPAGPDGLRPFTRESLAAIEQRISEERARNTKDYKADPGDVEEPKPRADLEVGKV
LPRIFGEIPAGLVGVPLEDIDPFYFRNQKTFIVLNKGKAIFRFSATSALYIFSPFHCIRR
ISIRILVHSLFSLFIMCTILTNCCFMAMSDPPLWTKYLEYTFTGIYTFESLIKILARGFC
TECFTFLRDPWNWLDFSVIVMAYVTEFVDLGNV. . . (+1719)

Figure 22: *scn5Laa* gene F0 Mutant#1, in-frame mutation. Mutant # 1 shows 6 bp deletion (in-frame mutation) compared to WT strand. The mutant is missing isoleucine and valine from its protein product compared to WT protein production.

GGATTTCAGTGTCATCGTCATGG (wt)

GGATTTCAGTGTCATCG---TGG (-3)

1931 aa. Missing Methionine (201st aminoacid)

MATMLLPAGPDGLRPFTRESLAAIEQRISEERARNTKDYKADPGDVEEPKPRADLEVGKV
LPRIFGEIPAGLVGVPLEDIDPFYFRNQKTFIVLNKGKAIFRFSATSALYIFSPFHCIRR
ISIRILVHSLFSLFIMCTILTNCCFMAMSDPPLWTKYLEYTFTGIYTFESLIKILARGFC
TECFTFLRDPWNWLDFSVIV-AYVTEFVDLGNV. . . (+1719)

WT Scn5Laa, 1932 aa

MATMLLPAGPDGLRPFTRESLAAIEQRISEERARNTKDYKADPGDVEEPKPRADLEVGKV
LPRIFGEIPAGLVGVPLEDIDPFYFRNQKTFIVLNKGKAIFRFSATSALYIFSPFHCIRR
ISIRILVHSLFSLFIMCTILTNCCFMAMSDPPLWTKYLEYTFTGIYTFESLIKILARGFC
TECFTFLRDPWNWLDFSVIVMAYVTEFVDLGNV. . . (+1719)

Figure 23: *scn5Laa* gene F0 Mutant#42, in-frame mutation. Mutant # 42 shows 3 bp deletion (in-frame mutation) compared to WT strand. The mutant is missing methionine from its protein product compared to WT protein production.

```
GGATTTCAGTGTCATCGTCATGG              (wt)

GGATTTCAGTG------TCATGG              (-6)
```

1930 aa. Missing Isoleucine and valine (199-200 aminoacids)

```
MATMLLPAGPDGLRPFTRESLAAIEQRISEERARNTKDYKADPGDVEEPKPRADLEVGKV
LPRIFGEIPAGLVGVPLEDIDPFYFRNQKTFIVLNKGKAIFRFSATSALYIFSPFHCIRR
ISIRILVHSLFSLFIMCTILTNCCFMAMSDPPLWTKYLEYTFTGIYTFESLIKILARGFC
TECFTFLRDPWNWLDFSV—MAYVTEFVDLGNV. . . (+1719)
```

WT Scn5Laa, 1932 aa

```
MATMLLPAGPDGLRPFTRESLAAIEQRISEERARNTKDYKADPGDVEEPKPRADLEVGKV
LPRIFGEIPAGLVGVPLEDIDPFYFRNQKTFIVLNKGKAIFRFSATSALYIFSPFHCIRR
ISIRILVHSLFSLFIMCTILTNCCFMAMSDPPLWTKYLEYTFTGIYTFESLIKILARGFC
TECFTFLRDPWNWLDFSVIVMAYVTEFVDLGNV. . . (+1719)
```

Figure 24: *scn5Laa* gene F0 Mutant#44, in-frame mutation. Mutant # 44 shows 6 bp deletion (in-frame mutation) compared to WT strand. The mutant is missing isoleucine and valine from its protein product compared to WT protein production.

```
GGATTTCAGTGTCATCGTCATGG              (wt)

GGATTTCAGTGTCA---TCATGG              (-3)
```

1931 aa. Missing valine (200th aminoacid)

```
MATMLLPAGPDGLRPFTRESLAAIEQRISEERARNTKDYKADPGDVEEPKPRADLEVGKV
LPRIFGEIPAGLVGVPLEDIDPFYFRNQKTFIVLNKGKAIFRFSATSALYIFSPFHCIRR
ISIRILVHSLFSLFIMCTILTNCCFMAMSDPPLWTKYLEYTFTGIYTFESLIKILARGFC
TECFTFLRDPWNWLDFSVI-MAYVTEFVDLGNV. . . (+1719)
```

WT Scn5Laa, 1932 aa

```
MATMLLPAGPDGLRPFTRESLAAIEQRISEERARNTKDYKADPGDVEEPKPRADLEVGKV
LPRIFGEIPAGLVGVPLEDIDPFYFRNQKTFIVLNKGKAIFRFSATSALYIFSPFHCIRR
ISIRILVHSLFSLFIMCTILTNCCFMAMSDPPLWTKYLEYTFTGIYTFESLIKILARGFC
TECFTFLRDPWNWLDFSVIVMAYVTEFVDLGNV. . . (+1719)
```

Figure 25: *scn5Laa* gene F0 Mutant#49, in-frame mutation. Mutant # 49 shows 3 bp deletion (in-frame mutation) compared to WT strand. The mutant is missing valine from its protein product compared to WT protein production.

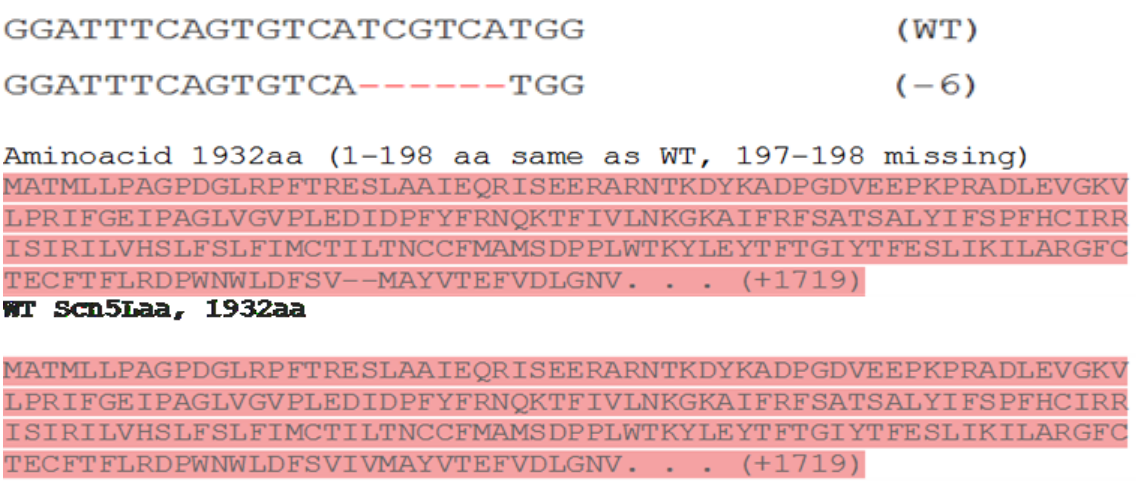

Figure 26: *scn5Laa* gene F0 Mutant#52, in-frame mutation. Mutant # 52 shows 6 bp deletion (in-frame mutation) compared to WT strand. The mutant is missing isoleucine and valine from its protein product compared to WT protein production.

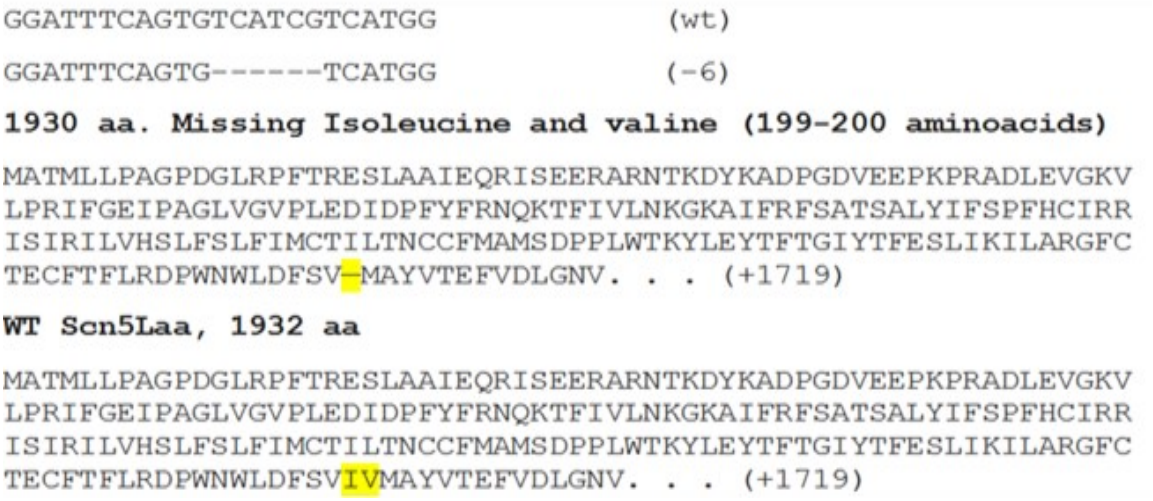

Figure 27: *scn5Laa* gene F0 Mutant#55, in-frame mutation. Mutant # 55 shows 6 bp deletion (in-frame mutation) compared to WT strand. The mutant is missing isoleucine and valine from its protein product compared to WT protein production.

```
GGATTTCAGTGTCATCGTCATGG              (wt)

GGATTTCAGTGTCATCG---TGG              (-3)
```
1931 aa. Missing Methionine (201st aminoacid)

```
MATMLLPAGPDGLRPFTRESLAAIEQRISEERARNTKDYKADPGDVEEPKPRADLEVGKV
LPRIFGEIPAGLVGVPLEDIDPFYFRNQKTFIVLNKGKAIFRFSATSALYIFSPFHCIRR
ISIRILVHSLFSLFIMCTILTNCCFMAMSDPPLWTKYLEYTFTGIYTFESLIKILARGFC
TECFTFLRDPWNWLDFSVIV-AYVTEFVDLGNV. . . (+1719)
```

WT Scn5Laa, 1932 aa

```
MATMLLPAGPDGLRPFTRESLAAIEQRISEERARNTKDYKADPGDVEEPKPRADLEVGKV
LPRIFGEIPAGLVGVPLEDIDPFYFRNQKTFIVLNKGKAIFRFSATSALYIFSPFHCIRR
ISIRILVHSLFSLFIMCTILTNCCFMAMSDPPLWTKYLEYTFTGIYTFESLIKILARGFC
TECFTFLRDPWNWLDFSVIVMAYVTEFVDLGNV. . . (+1719)
```

Figure 28: *scn5Laa* gene F0 Mutant#32, in-frame mutation.
Mutant # 32 shows 3 bp deletion (in-frame mutation) compared to WT strand. The mutant is missing methionine from its protein product compared to WT protein production.

```
GGATTTCAGTGTCATCGTCATGG              (wt)

GGATTTCAGTGTCA---TCATGG              (-3)
```

1931 aa. Missing valine (200th aminoacid)

```
MATMLLPAGPDGLRPFTRESLAAIEQRISEERARNTKDYKADPGDVEEPKPRADLEVGKV
LPRIFGEIPAGLVGVPLEDIDPFYFRNQKTFIVLNKGKAIFRFSATSALYIFSPFHCIRR
ISIRILVHSLFSLFIMCTILTNCCFMAMSDPPLWTKYLEYTFTGIYTFESLIKILARGFC
TECFTFLRDPWNWLDFSVI-MAYVTEFVDLGNV. . . (+1719)
```

WT Scn5Laa, 1932 aa

```
MATMLLPAGPDGLRPFTRESLAAIEQRISEERARNTKDYKADPGDVEEPKPRADLEVGKV
LPRIFGEIPAGLVGVPLEDIDPFYFRNQKTFIVLNKGKAIFRFSATSALYIFSPFHCIRR
ISIRILVHSLFSLFIMCTILTNCCFMAMSDPPLWTKYLEYTFTGIYTFESLIKILARGFC
TECFTFLRDPWNWLDFSVIVMAYVTEFVDLGNV. . . (+1719)
```

Figure 29: *scn5Laa* gene F0 Mutant#34, in-frame mutation. Mutant # 34 shows 3 bp deletion (in-frame mutation) compared to WT strand. The mutant is missing valine from its protein product compared to WT protein production.

Scn5Laa F0 Mutant#7

GGATTTCAGTGTCATCGTCATGG (wt)

GGATTTCAGTGTCACTGGCTGGATTTCAGTGTCAAACTCATGG (−3/+23)

Aminoacid 210aa (1-198 aa same as WT, 199-210 aa changed)

MATMLLPAGPDGLRPFTRESLAAIEQRISEERARNTKDYKADPGDVEEPKPRADLEVGKV
LPRIFGEIPAGLVGVPLEDIDPFYFRNQKTFIVLNKGKAIFRFSATSALYIFSPFHCIRR
ISIRILVHSLFSLFIMCTILTNCCFMAMSDPPLWTKYLEYTFTGIYTFESLIKILARGFC
TECFTFLRDPWNWLDFSVTGWISVSNSWRM−stop

WT Scn5Laa, 1932 aa

MATMLLPAGPDGLRPFTRESLAAIEQRISEERARNTKDYKADPGDVEEPKPRADLEVGKV
LPRIFGEIPAGLVGVPLEDIDPFYFRNQKTFIVLNKGKAIFRFSATSALYIFSPFHCIRR
ISIRILVHSLFSLFIMCTILTNCCFMAMSDPPLWTKYLEYTFTGIYTFESLIKILARGFC
TECFTFLRDPWNWLDFSVIVMAYVTEFVDLGNV. . . (+1719)

Figure 30: *scn5Laa* F0 Mutant#7, frameshift mutation. Mutant # 7 shows 3 bp deletion and 23 bp insertion (frameshift mutation) compared to WT strand. The mutant has 1-198 same amino acids as the WT protein product. However, amino acids 199-210 are changed as highlighted in yellow. The protein product of this mutant is only 210 amino acids compared to WT protein product of 1932 amino acids.

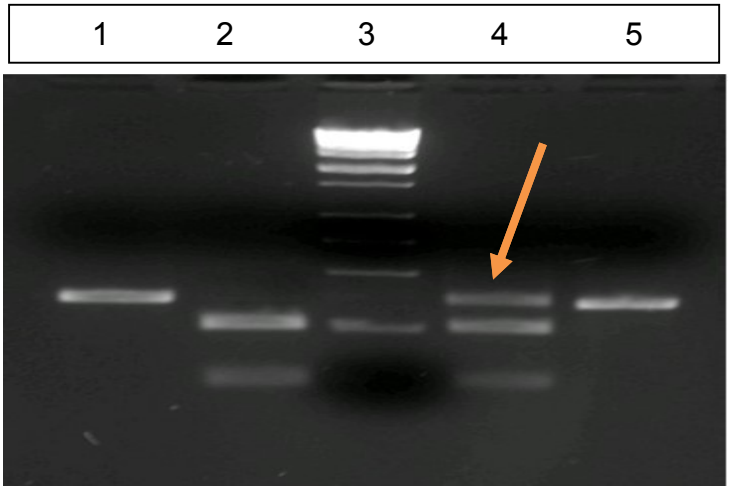

Figure 31: Gel Image to show *scn5Lab* mutation in F0 Generation embryos microinjected with TALENs. Lane 1 and 5 show *scn5Lab* undigested and WT control, respectively representing a single band at 361 bp. Lane 2 shows WT PCR product digested with *Apa*I showing two bands at 310 bp and 104 bp indicating no sign of indel mutation in the spacer region of the TALENs targeted site. Lane 4 contains samples from bulk screening of 30 microinjected embryos digested with *Apa*I. Lane 4 shows bands at 361 bp, 310 bp, and 104 bp. The band at 361 bp represents undigested mixture indicating the presence of indel mutation.

CCTGGCGCGGGGTTTCTGCATCGGGCCCTTCACATTTCTGAGGGACCCCTGGA (WT)

(1) CCTGGCGCGGGGTTTCTGCATCGGGCCGCCCTTCACATTTCTGAGGGACCCCTGGA (+4)

(2) CCTGGCGCGGGGTTTCT----------CACATTTCTGAGGGACCCCTGGA (-13)

(4) CCTGGCGCGGGGTTTCTGCATCGGGCTCTTCACATTTCTGAGGGACCCCTGGA (SNP)

Figure 32: Sequencing results of *scn5Lab* F0 generation. The highlighted portion refers to *scn5Lab* TALENs forward and reverse binding sites targeted from plasmid *scn5Lab* PEAS-TALENs and PERR-TALENs, respectively. Clone #1 shows 4 bp insertion compared to WT strand. Clone # 2 and 4 show 13 bp deletion and single nucleotide polymorphism compared to WT strand.

GAAGATGGCAGCCATACTGTTTCCACCGGGTCCTGA (WT)

(3) GAAGATGGCAGCCATACTGTTTCATTCAGACACCGGGTCCTGA (+7)

(5) GAAGATGGCAGCCATACTGTTTCTGGACACCGGGTCCTGA (+6/−2)

Figure 33: Sequencing results of *scn5Lab* Bulk Screening (CRISPR-CAS9). The highlighted portion in yellow refers to 23 bp CRIPSR target site for *scn5Lab.* Clone # 3 shows 7 bp insertion compared to WT strand. Clone # 5 shows 6 bp insertion and 2 bp deletion compared to WT strand.

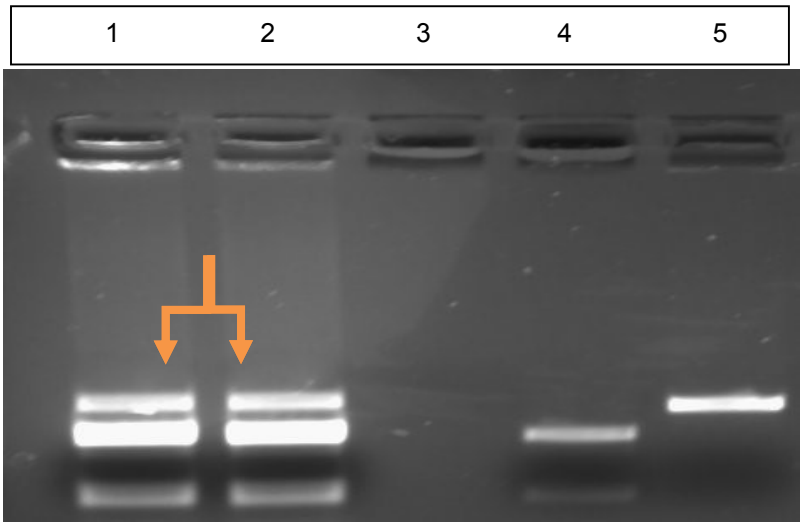

Figure 34: *scn5Lab* Male #3-8 F0 generation Mutation. Lanes1-2 represent PCR product of *scn5Lab* mutant #3 digested with *Apa*I. The upper band matches the undigested control shown in lane 5 producing band at 361 bp. This band shows presence of indel mutation in lanes 1-2. Second and third bands in lanes 1-2 are 310 bp and 104 bp long. Lane 4 shows WT PCR product digested with *Apa*I, producing two bands at 310 bp and 104 bp.

```
Scn5lab F0 Mutant#3
CCTGGCGCGGGGTTTCTGCATCGGGCCCTTCACATTTCTGAGGGACCCCT      (WT)
CCTGGCGCGGGGTTTCTGCAT-----TCTTCACATTTCTGAGGGACCCCT      (-6/+1)

Aminoacid 203 aa (1-181 same as wt, 182-203 changed)
MAAILFPPGPDSLHRFTRESLAGIEQRIAEEEARNAKRYQEDRGDVEPPKPRADLEAGKQLPR
IFGDIPSALVGVPLEDIDPFYFQNRRTFIVLNKGKAIFRFSATSALYIFSPFHPIRRASIRIL
VHSLFSLFIMCTILTNCCFMAMSEPAQWAKYVEYTFTGIYTFESLIKILARGFCILHISEGPL
ELAGFQCDSDGICN-stop
WT 1954aa
MAAILFPPGPDSLHRFTRESLAGIEQRIAEEEARNAKRYQEDRGDVEPPKPRADLEAGKQLPR
IFGDIPSALVGVPLEDIDPFYFQNRRTFIVLNKGKAIFRFSATSALYIFSPFHPIRRASIRIL
VHSLFSLFIMCTILTNCCFMAMSEPAQWAKYVEYTFTGIYTFESLIKILARGFCIGPFTFLRD
PWNWLDFSVILMAYV...(+1750)
```

Figure 35: *scn5Lab* Male #3-8 F0 Frameshift Caused by Indel Mutation. Mutant # 3-8 shows 6 bp deletion and 1 bp insertion (frameshift mutation) compared to WT strand. The mutant has 1-181 same amino acids as the WT protein product. However, amino acids 182-203 are changed as highlighted in yellow. The protein product of this mutant is only 203 amino acids long compared to WT protein product of 1954 amino acids.

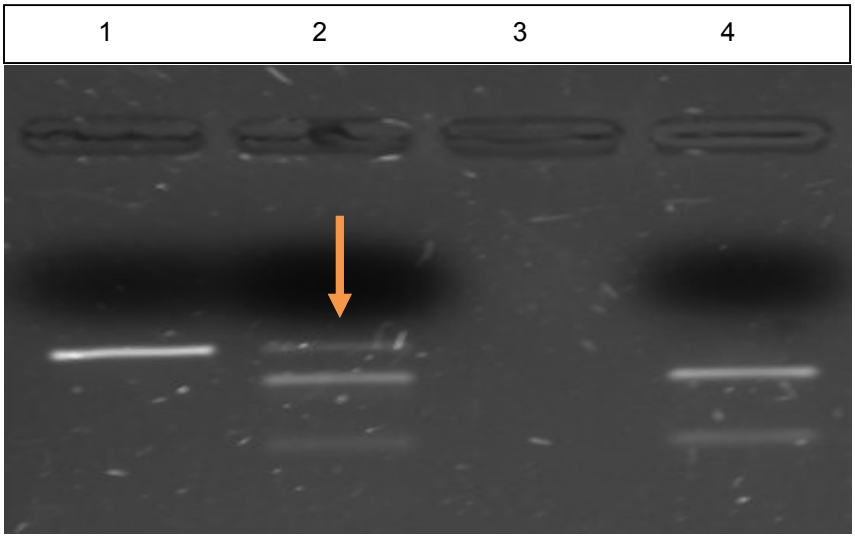

Figure 36: *scn5Lab* Male #5-6 F0 generation Mutation. Lane 1 represents undigested control at 361 bp. Lane 2 represent PCR product of *scn5Lab* mutant #5 digested with *Apa*I. The upper band matches the undigested control shown in lane 1 producing band at 361 bp. This band shows presence of indel mutation in lanes 2. Second and third bands in lanes 1-2 are 310 bp and 104 bp long which matches with lane 4. Lane 4 shows WT PCR product digested with *Apa*I producing two bands at 310 bp and 104 bp.

```
Scn5lab F0 Mutant#5
CCTGGCGCGGGGTTTCTGCATCGGGCCCTTCACATTTCTGAGGGACCCCT      (WT)
CCTGGCGCGGGGT---------------TTCACATTTCTGAGGGACCCCT      (-15)

Aminoacid 204 aa (1-179 same as wt, 180-184 missing)
MAAILFPPGPDSLHRFTRESLAGIEQRIAEEEARNAKRYQEDRGDVEPPKPRADLEAGKQLPR
IFGDIPSALVGVPLEDIDPFYFQNRRTFIVLNKGKAIFRFSATSALYIFSPFHPIRRASIRIL
VHSLFSLFIMCTILTNCCFMAMSEPAQWAKYVEYTFTGIYTFESLIKILARGF-----TFLRD
PWNWLDFSVILMAYV...(+1750)
WT 1954aa
MAAILFPPGPDSLHRFTRESLAGIEQRIAEEEARNAKRYQEDRGDVEPPKPRADLEAGKQLPR
IFGDIPSALVGVPLEDIDPFYFQNRRTFIVLNKGKAIFRFSATSALYIFSPFHPIRRASIRIL
VHSLFSLFIMCTILTNCCFMAMSEPAQWAKYVEYTFTGIYTFESLIKILARGFCIGPFTFLRD
PWNWLDFSVILMAYV...(+1750)
```

Figure 37: *scn5Lab* Male #5-6 F0 In-frame Mutation.
Mutant # 5 shows 15 bp deletion (in-frame mutation) compared to WT strand. The mutant is missing cysteine, isoleucine, glycine, proline, and phenyalanine at positions 180-184 compared to the WT protein product.

Scn5Lab F0 Mutant #21

GGCAGCCATACTGTTTCCACCGG (WT)
GGCAGCCATACTGTTCCTGACAGTCTGCACCGG (+11,2SNP)

Aminoacid 13 aa (1-6 same as wt, 7-13 aa changed)

MAAILFLTVCTGS-stop

WT 1954 aa

MAAILFPPGPDSLHRFTRESLAGIEQR. . . (+1927)

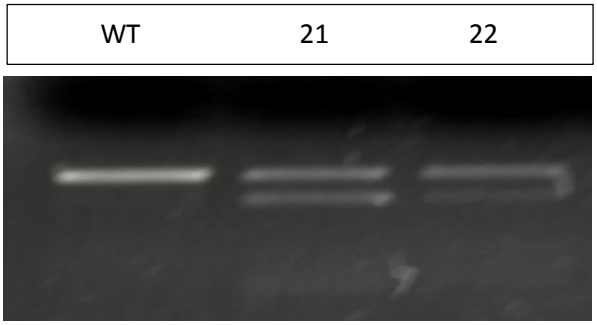

Figure 38: *scn5Lab* F0 CRISPR-CAS9 Mutant#21, frameshift mutation. Mutant # 21 shows 11 bp insertion (frameshift mutation) compared to WT strand. The mutant has the same first six amino acids as WT. Amino acids 7-13 are changed due to frameshift in the coding sequence (highlighted in yellow). The final protein product of the mutant is 13 amino acids compared to 1954 amio acid of WT protein. The gel image shows samples for mutant #21 and 22 after T7 endonuclease digestion. Lane 1 shows WT undigested control representing band at 351 bp. Lanes 2-3 produced three bands, at 351bp, 271 bp, and 79bp compared to WT strand. The upper band represents undigested mixture while the last two bands represent successful T7 endonuclease digestion.

Scn5Lab F0 Mutant #22

GGCAGCCATACTGTTTCCACCGG (WT)
GGCAGCCATACTGTTTCGGGTCCTGACAGTCTGCACCGG (+16)

Aminoacid 15 aa (1-6 same as wt, 7-15 aa changed)

MAAILFRVLTVCTGS-stop

WT 1954 aa

Figure 39: *scn5Laa* F0 CRISPR-CAS9 Mutant#22, frameshift mutation. Mutant # 22 shows 16 bp insertion (frameshift mutation) compared to WT strand. The mutant has the same first six amino acids as WT. Amino acids 7-15 are changed due to frameshift in the coding sequence (highlighted in yellow). The final protein product of the mutant is 15 amino acids compared to 1954 amio acid of WT protein.

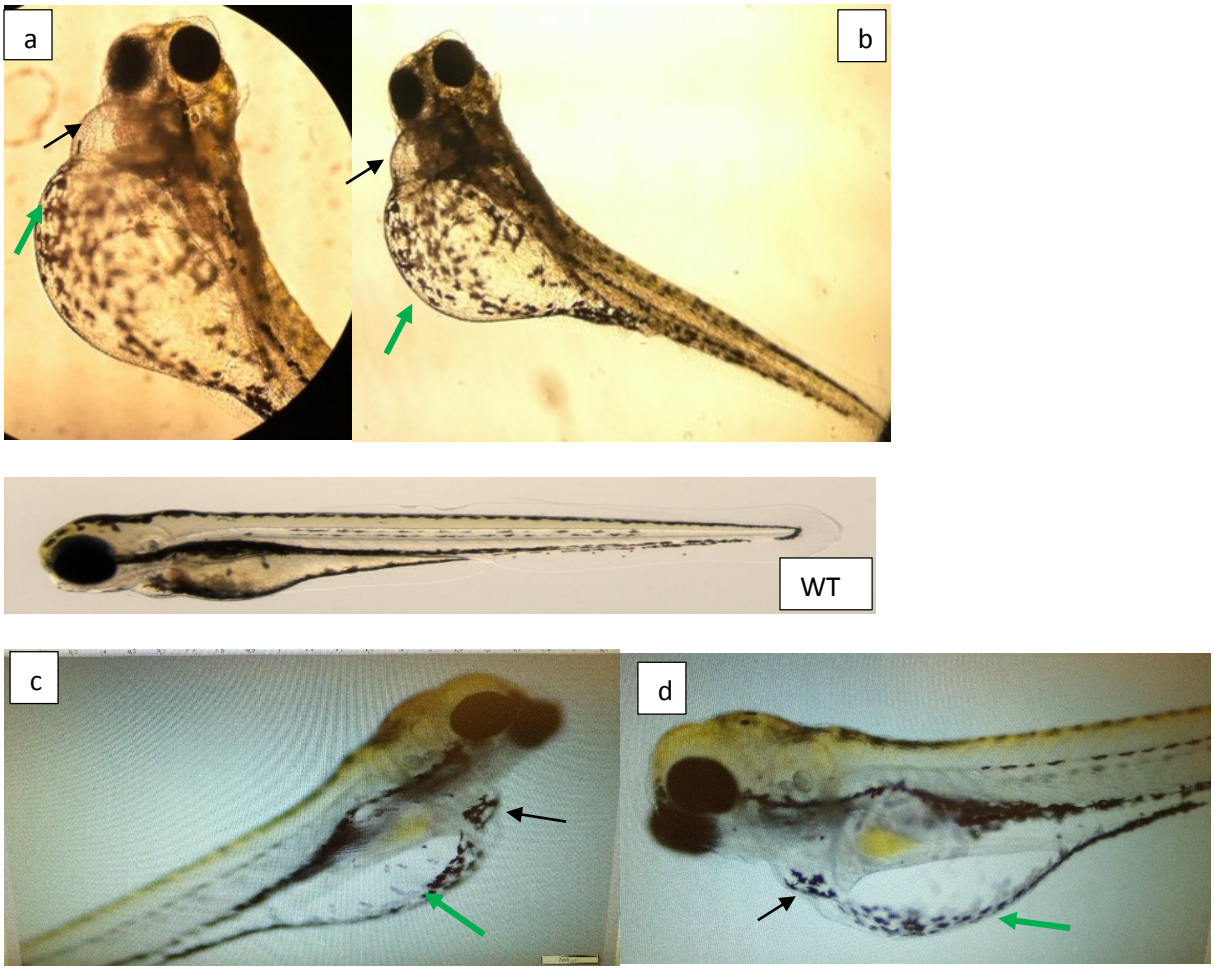

Figure 40: *scn5Lab* F2 generation embryos showing abnormal phenotypes. The figure above shows various developmental defects in F2 generation homozygous null allele *scn5Lab* mutants compared to wild-type (WT) embryos at 6dpf. Black arrow shown in images a-d indicate cardiac edema compared to WT embryos. Green arrows in images a-d indicate yolk-sac edema compared to WT embryo.

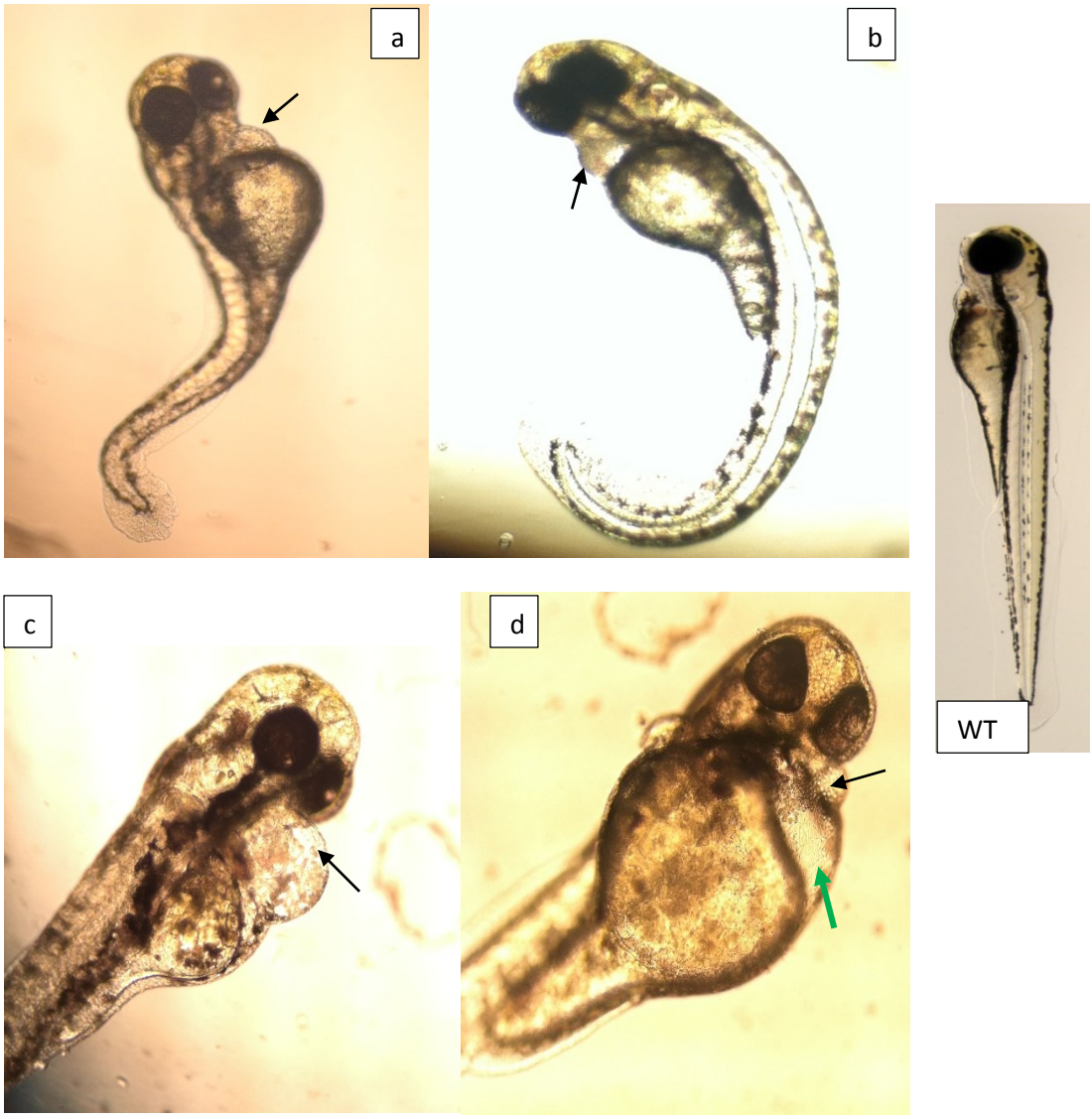

Figure 41: *scn5Laa* embryos showing defective phenotypes post microinjection. The Figure above shows various developmental defects in F0 generation embryos after *scn5Laa* CRISPR-CAS9 gRNA microinjections compared to wild-type (WT) embryos from 50-80hpf. Black arrow shown in images a-d indicate cardiac edema compared to WT embryos. Green arrow in image d indicate yolk-sac edema compared to WT embryo. Curvature of the spine is seen in images a and b.

hpf	*scn5Laa* F1	*scn5Laa* F2	*scn5Lab* F1	*scn5Lab* F2	WT
26 hpf	32	30	31	31	33
28 hpf	46	43	45	43	46
31 hpf	57	56	57	56	61
49 hpf	127	120	124	125	127
51 hpf	144	144	146	147	149
53 hpf	140	142	145	149	148
55 hpf	145	148	147	151	151

Table 10: Heartbeat Rate per minute. The above table shows heartbeat per minute of heterozygous (*scn5Laa* F1 and *scn5Lab* F1), homozygous (*scn5Laa* F2 and *scn5Lab* F2), and WT embryos at 26, 28, 31, 49, 51, 53, and 55 hpf.

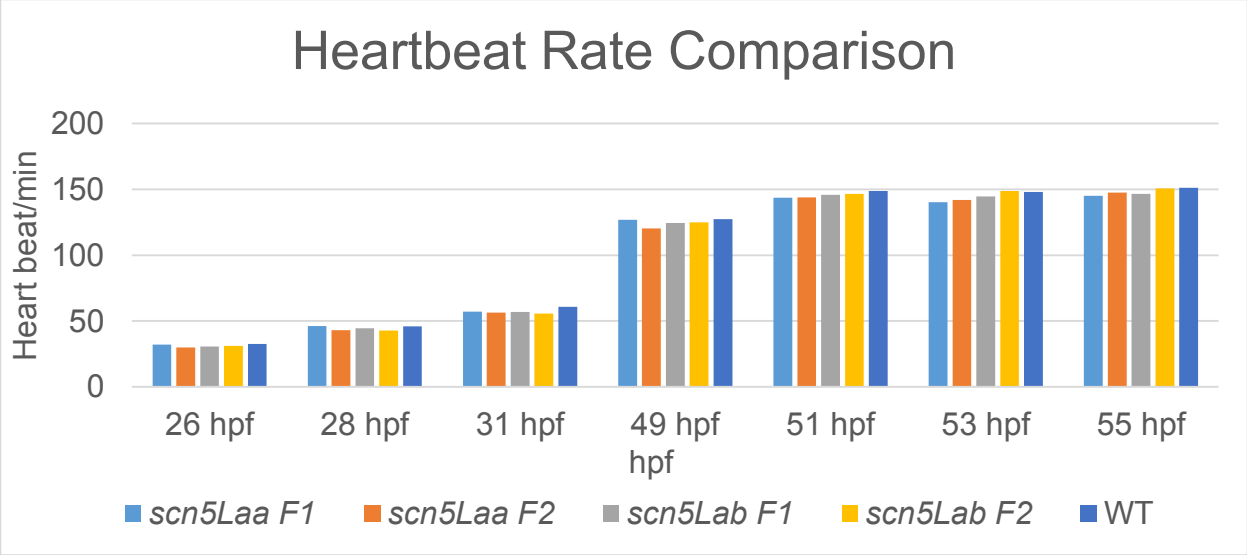

Figure 42: Heartbeat Rate comparisons. The above graph compares the heart rate of *scn5Laa* heterozygous (F1) and homozygous embryos (F2) to *scn5Laa* heterozygous (F1) and homozygous embryos (F2) and WT embryos at 26, 28, 31, 49, 51, 53, and 55 hpf.

CHAPTER 4: DISCUSSION

Based on the heart developmental defects induced by antisense morpholino oligonucleotide (MO) gene knockdown of zebrafish genes *scn5Laa* and *ab* reported by Chopra et al., and assuming that these gene knockdown phenotypes were not the result of MO off target or toxicity effects**, it was hypothesized that both the TALENs and CRISPR-CAS9-induced knockout mutations in the zebrafish *scn5Laa* and *ab* genes would phenocopy the developmental defects induced by MO's directed against *scn5Laa* and *ab* by Chopra et al.** (Chopra et al. 2010). To test the hypothesis that knockout of the zebrafish *scn5Laa* and *ab* genes would result in heart developmental defects characterized by cardiac and yolk sac edema, cardiac arrhythmia, and progressive heart deterioration, knockout mutation-bearing zebrafish lines of these genes were constructed. The specific TALENs and CRISPR-CAS9 genome editing-induced knockout mutations in these lines were characterized as frameshift mutations that induced premature translation termination codons in gene-transcribed mRNAs that could further lead to truncation of the proteins early in translation, yielding severely shortened proteins lacking even the first functional transmembrane coding domains. Heterozygous and homozygous frame-shift mutants from each mutant-bearing line showed that zebrafish embryos from these lines developed normally compared to wild-type control embryos. These results provide evidence that the *scn5Laa* and *ab* encoded proteins independently do not play a role in specification of embryonic heart development and suggest that the developmental defects produced by individual antisense MO treatment of zebrafish embryos do not result from direct knockdown of either *scn5Laa* or *scn5Lab*-derived mRNAs individually

as reported by Chopra (2008) and Chopra et al (2010). Based on these results, we reject the hypothesis that *scn5Laa* or *ab* gene-coded proteins independently act to specify normal zebrafish embryonic heart development.

While the results from TALENs and CRISPR-CAS9 induced knockout of zebrafish *scn5Laa* and *ab* genes did not lead to the hypothesized developmental defects, there are a number of possible explanations to account for the observed results. A likely explanation based on the nature of antisense MOs and the close sequence relationship and potential overlapping subfunctions between the *scn5Laa* and *ab,* is that treatment with MOs directed toward individual gene-derived mRNAs from either *scn5Laa* or *ab* may have inhibited the translation of both mRNAs and that dual knockdown is required to induce developmental defects. The MOs used by Chopra (2008) and Chopra et al. (2010) to knockdown post-transcriptional RNA splicing and mRNA translation of *scn5Laa* and *ab* included MOs directed toward the translational initiation start sites and splice junctions for both genes. All the MOs used by Chopra (2008) and Chopra et al. (2010) induced the stereotypical heart developmental defects described in this thesis, including those linked to specific alleles in the human *SCN5A* gene. Despite the differences in their target sites and modes of action, it is possible that the knockdown of either *scn5Laa* or *ab* independently affects the function of the other gene in relation to normal heart development. If this is the case, then it is possible we did not observe an effect of individual *scn5Laa* or *ab* knockouts because independent knockouts of each gene alone is insufficient to induce heart defects like those observed by Chopra (2008) and Chopra et al. (2010). A test of this hypothesis will await the construction of double knockouts for both *scn5Laa* and *ab* in zebrafish. Double

knockout mutants derived by intercrossing homozygous single knockouts for both *scn5Laa* and *ab* are being constructed in the laboratory and results from these crosses are forthcoming.

It is also possible that the homozygous knockouts for *scn5Laa* or *ab*, while verified for frameshift mutations leading to premature translation termination sites in *scn5Laa* or *ab*-encoded mRNA at the TALENs and CRISPR-CAS9 target sites, still produce functional protein products and so do not show the hypothesized developmental defects. This result could occur if there were compensatory frameshift mutants induced near, but downstream, of the verified frameshifts. By compensatory, it means that these frameshifts would return the mRNA coding sequence back to the original reading frame but at a site distant from intended and sequenced target site mutation. The resultant mRNA would encode a protein with a series of frameshifted amino acids between the verified TALENs and CRISPR-CAS9-induced frameshifts and the compensatory 2nd site frameshift but with a wild-type amino acid sequence downstream of the compensatory frameshift that would return the mRNA to the proper reading frame. The net effect of the compensatory frameshift would be to generate a protein product with an amino acid sequence comparable to wild-type with the exception of the amino acids encoded by the region of the mRNA bordered by the upstream and downstream frameshifts. While this explanation may seem highly unlikely, given the spontaneous frequency of frameshift mutations, little is known about off-target effects of TALENs and CRISPR-CAS9-induced mutations, including those near the editing target site. The likelihood for such an explanation is more probable if there is strong selection against knockouts for these two genes. Evidence from mouse and human mutations in

the zebrafish orthologs of the human and mouse *SCN5A* gene suggest that homozygotes of certain alleles suffer embryonic lethality (Nuyens et al. 2001; Papadatos et al. 2002; Lei et al. 2005). In fact, results from this thesis suggest that knockouts of *scn5Laa*, in particular, are highly enriched for in-frame mutations (12/13 or 92%) relative to out-of-frame (1/13 or 8%), frameshifting mutations in adult survivors of TALENs and CRISPR-CAS9 treatment. An excess of in-frame mutations in adult survivors would be expected if nonsense mutation-inducing frameshift mutations resulted in a preponderance of prematurely terminated protein products leading to embryonic lethality. Based on statistical probability, the likelihood of frameshift mutations early in the mRNA coding sequence of these two genes leading to premature termination sequences resulting in nonfunctional protein products being far greater than small in-frame mutations having similar effects, is very significant. The isolation of a comparable number of frameshift relative to in-frame mutations in bulk screening of F0 TALENs-treated embryos (Figure 15) in contrast to a complete absence of frame-shift mutations in surviving adult F0 fish, argues that there is a strong selection against frame-shift mutations in the sites targeted. These results further argue that surviving frameshifted knockouts may not truly inactive the generation of a functional protein product. There are several ways to determine whether the 'compensatory' 2nd site frameshift hypothesis can explain the observed results. Reverse transcription and sequencing of the cDNA derived from mRNA prepared from homozygous frameshifted knockouts would reveal whether compensatory mutations downstream from the TALENs and CRISPR-CAS9-induced mutations are present. This approach would provide direct information concerning the location of the compensatory frameshift as

well as the exact nature of the deduced changes in the amino acid sequences of the coding region between the upstream and downstream frameshifts. An alternative and related but more time-consuming approach would be to sequence the PCR amplified genomic DNA corresponding to the exons of the gene. These results would provide the same information as the cDNA sequencing. Another alternative is to determine whether a protein product is being synthesized and, if so, whether the protein is truncated, full length or slightly modified. This approach requires the availability of highly specific antibody for western blot analysis. While antibodies directed toward human *SCN5A* are commercially available, they have not been demonstrated to be specific either for human or zebrafish *scn*5 gene family members.

There is also a possibility, given that protein product of both *scn5Laa* and *ab* are more than 1900 amino acids long, that translation initiates again at an ATG codon downstream of the frameshifted region in both scn5Laa and ab knockouts. This would make the protein product of the knockouts exactly the same as WT except from the frameshifted region through the secondary ATG codon. This would explain why none of our mutants showed expected developmentally defective phenotype. Western blot analysis with highly specific antibody will confirm if some other ATG codon downstream of the presumed initiator, a secondary site, is the source of protein product frameshifted mutants.

Concerns about the potential lethality of *scn5Laa* knockouts, in particular, but also about *scn5Lab* knockouts prompted a series of experiments designed to examine the lethality and developmental defects in F0 stage zebrafish embryos microinjected with CRISPR-CAS9-targeting mRNAs directed toward *scn5Laa*. Results from these

experiments proved interesting but inconclusive. We constantly observed 25-35% death of the developing embryos injected with *scn5Laa* gRNA compared to 5-7% death among embryos in the control group. There was evidence for an excess of embryo mortality and developmental defect (3-10%) induction for microinjections of CRISPR-CAS9-targeting mRNAs directed toward *scn5Laa* compared to control CRISPR-CAS9 targeting other genes in the genome. However, isolation and characterization of DNA from developmentally defective F0 embryos revealed that the targeted sites were not mutated, at least at levels detectable based on sequence analysis of target site PCR-amplified genomic DNA. These results suggest that either the embryos exhibited developmental defects and excessive mortality compared to microinjected controls because of deleterious but undetectable mutations in *scn5Laa* or that the targeting CRISPR-CAS9 mRNA directed to *scn5Laa* was differentially toxic to embryos relative to the control CRISPR-CAS9 mRNA. It is not clear how to experimentally differentiate between these alternative explanations.

It is also possible that Chopra (2008) and Chopra et al.'s knockdown treatments affected the translation of other Na^+ ion channel family gene targets and that the combined effects generated their observed cardiac developmental defects. If this is the case, then genome-editing knockouts of other Na^+ ion channel would have to be constructed and examined for their effects on zebrafish embryonic development. This explanation is considered very unlikely because it does not account for the effects observed for transgenic zebrafish bearing mutant alleles of the human *SCN5A* gene.

As a final note, it is interesting that the construction of transgenic zebrafish with an integrated copy of a human *SCN5A* gene bearing an allele strongly linked to defects

in human heart function, *SCN5A-D1275N*, showed defects in zebrafish embryonic development similar to those reported by Chopra (2008) and Chopra et al. (2010). Moreover, these transgenic zebrafish showed increased embryonic mortality compared to transgenic zebrafish bearing the wild-type human *SCN5A* gene and to wild-type zebrafish. However, transgenic zebrafish lines with the human *SCN5A-D1275N*-bearing gene, showed incomplete penetrance of phenotype among the fish examined as did humans with this allelic form of *SCN5A*. These results are indicative of the sensitive nature and activity of allelic variants of *SCN5A* and may reflect the sensitivity of developmental phenotypes to variation in expression of this class of genes from humans and zebrafish.

REFERENCES

1. Baker, K., K.S. Warren, G. Yellen, M.C. Fishman. “Defective "pacemaker" current (Ih) in a zebrafish mutant with a slow heart rate.” *Proceedings of the National Academy of Sciences of the United States of America* 94.9 (1997):4554-4559.

2. Balser, J.R. “Inherited sodium channelopathies: novel therapeutic and proarrhythmic molecular mechanisms.” *Trends in Cardiovascular Medicine* 11.6 (2001):229-237.

3. Balser, J.R. “Sodium "channelopathies" and sudden death: must you be so sensitive?” *Circulation Research* 85.9 (1999):872-874.

4. Belair, C.D., R.E. Peterson, W. Heideman. “Disruption of erythropoiesis by dioxin in the zebrafish.” *Developmental Dynamics* 222 (2001):581–594.

5. Cade, L., D. Reyon, W.Y. Hwang, S.Q. Tsai, S. Patel, C. Khayter, J.K. Joung, J.D. Sander, R.T. Ptereson, J-R. J. Yeh. “Highly efficient generation of heritable zebrafish gene mutations using homo- and heterodimeric TALENs.” *Nucleic Acid Research* 40.16 (2012): 8001-8010.

6. Carls, M.G., L. Holland, M. Larsen, T.K. Collier, N.L. Scholz, J.P. Incardona. “Fish embryos are damaged by dissolved PAHs, not oil particles.” *Aquatic Toxicology* 88 (2008):121-127.

7. Carls, M.G., S.D. Rice, J.E.Hose. “Sensitivity of fish embryos to weathered crude oil: Part I. Low-level exposure during incubation causes malformations, genetic damage, and mortality in larval Pacific herring (Clupea pallasi).” *Environmental Toxicology and Chemistry* 18 (1999):481–493.

8. Catterall, W.A., A.L. Goldin, S.G. Waxman. “International Union of Pharmacology. XLVII. Nomenclature and structure-function relationships of voltage-gated sodium channels.” *Pharmacological Reviews* 57.4 (2005):397-409.

9. "Chen and Wente Lab CRISPR Plasmids Available from Addgene." *Addgene: Chen and Wente Labs CRISPR Plasmids*. <https://www.addgene.org/crispr/chen/>

10. Chopra, Sameer. *Sodium Channels are required for Cardiac Cell-Fate Specification Via a Novel, non-electrogenic Mechanism in zebrafish.* Ph.D. dissertation, Vanderbilt University, 2008.

11. Chopra, S., D.M. Stroud, H. Watanabe, J.S. Bennett, C.G. Burns, K.S. Wells, K.S., T. Yang, T.P. Zhong, and D.M. Roden. “Voltage-Gated Sodium Channels Are Required for Heart Development in zebrafish.” *Circulation Research* 106 (2010):1342-1350.

12. Chopra, S., H. Watanabe, T.P. Zhong, D.M. Roden. “Molecular cloning and analysis of zebrafish voltage-gated sodium channel beta subunit genes: implications for the evolution of electrical signaling in vertebrates.” Journal of Evolutionary Biology 7.113 (2007).

13. Crone, T.J., M. Tolstoy. “Magnitude of the 2010 Gulf of Mexico oil leak.” *Science* 2010:330-634.

14. Dahlem, T.J., K. Hoshijima, M. J. Jurynec, D. Gunther; C.G. Starker, A.S. Locke, A.M. Weis, D.F. Voytas, D.J. Grunwald. “Simple Methods for Generating and Detecting Locus-Specific Mutations Induced with TALENs in the zebrafish Genome.” *PLOS Genetics* 8.8 (2012): e1002861.

15. de Soysa, T. Y., A. Ulrich, T. Friedrich, D. Pite, S. L. Compton, D. Ok, R. L. Bernardos, G. B. Downes, S. Hsieh, R. Stein, M. C. Lagdameo, K. Halvorsen, L-R. Kesich, and M. JF. Barresi. “Macondo crude oil from the Deepwater Horizon Oil Spill Disrupts Specific Developmental Processes during zebrafish Embryogenesis” *Journal of Biology* 10:40 (2012) 1-24.

16. Deltcheva, E., K. Chylinski, C.M. Sharma, K. Gonzales, Y. Chao, Z.A. Pirzada, M.R. Eckert, J. Vogel, E. Charpentier. “CRISPR RNA maturation by trans-encoded small RNA and host factor RNase III.” *Nature* 471.7340 (2011):602–607.

17. Dumaine, R., Q. Wang, M.T. Keating, H.A. Hartmann, P.J. Schwartz, A.M. Brown, G.E. Kirsch. “Multiple mechanisms of Na+ channel--linked long-QT syndrome.” *Circulation Research* 78.5 (1996):916-924.

18. George, AL., Jr. “Inherited disorders of voltage-gated sodium channels.” *Journal of Clinical Investigation* 115.8 (2005):1990-1999.

19. Ghiassi, Erfaan. *The Effects of Crude Oil Exposure on Danio rerio (zebrafish) Embryonic Development.* Masters thesis, East Carolina University, 2014.

20. Goldin, A.L. “Resurgence of sodium channel research.” *Annual Review of Physiology* 63(2001):871-894.

21. Gurnett, C. A., K.P. Campbell. “Transmembrane auxiliary subunits of voltage-dependent ion channels.” *Journal of Biological Chemistry* 271(1996):27975–27978.

22. Guy, H. R., S.R. Durell. “Structural modes of Na+, Ca2+, and K+ channels.” *Society of General Physiology Series* 50(1995):1–16.

23. Heintz R. A., J.W. Short, S.D Rice. “Sensitivity of fish embryos to weathered crude oil: Part II. Increased mortality of pink salmon (Oncorhynchus gorbuscha)

embryos incubating downstream from weathered Exxon Valdez crude oil." *Environmental Toxicology and Chemistry* 18 (1999):494–503.

24. Henry, T.R., J.M. Spitsbergen, M.W. Hornung, C.C. Abnet, R.E. Peterson. "Early life stage toxicity of 2,3,7,8-tetrachlorodibenzo-pdioxin in zebrafish (Danio rerio)." *Toxicology and Applied Pharmacology* 142 (1997):56–68.

25. Herfst, L.J., M.B. Rook, H.J. Jongsma. "Trafficking and functional expression of cardiac Na+ channels." *Journal of Molecular and Cellular Cardiology* 36.2 (2004):185-193.

26. Hicken, C. E., T.L. Linbo, D. H. Baldwin, M.L. Willis, M.S. Myers, L. Holland, M. Larsen, M. S. Stekoll, S. D. Rice, T. K. Collier, N.L. Scholz, and J.P. Incardona "Sublethal Exposure to Crude Oil during Embryonic Development Alters Cardiac Morphology and Reduces Aerobic Capacity in Adult Fish." *Proceedings of the National Academy of Sciences* 108.17 (2011) 7086-7090.

27. Hong, K., J. Hu, J. Yu, R. Brugada. "Concomitant Brugada-like and short QT electrocardiogram linked to *SCN5A* mutation." *European Journal of Human Genetics* 20(2012):1189-1192.

28. Huang, P., A. Xiao, M. Zhou, Z. Zhu, S. Lin, and B. Zhang. "Heritable gene targeting in zebrafish using customized TALENs." *Nature Biotechnology* 29.8 (2011): 699-700.

29. Huttner, I.G., G. Trivedi, A. Jacoby, S.A. Mann, J.I. Vandenberg, D. Fatkin. 'A Transgenic zebrafish Model of a Human Cardiac Sodium Channel Mutation Exhibits Bradycardia, Conduction system abnormalities, and early death." *Journal of Molecular and Cellular Cardiology* 61 (2013):123-132.

30. Hwang, W.Y., F.U. Yanfang, R. Deepak, M.L. Maeder, S.Q. Tsai, J.D. Sander, R. T. Peterson,J.-R. J. Yeh, and J. K. Joung. (2013) "Efficient genome editing in zebrafish using a CRISPR-Cas system." *Nature Biotechnology* 31.3 (2013): 227-229.

31. Incardona, J.P., M.G. Carls, H. Teraoka, C.A. Sloan, T.K. Collier, N.L. Scholz. 'Aryl hydrocarbon receptor-independent toxicity of weathered crude oil during fish development." *Environmental Health Perspective* 113 (2005):1755-1762.

32. Incardona, J.P., T.K. Collier, N.L. Scholz. "Defects in cardiac function precede morphological abnormalities in fish embryos exposed to polycyclic aromatic hydrocarbons." *Toxicology and Applied Pharmacology* 196(2004):191-205.

33. Incardona, J.P., T.K. Collier, N.L. Scholz. "Oil spills and fish health: exposing the heart of the matter." *Journal of Exposure Science and Environmental Epidemiology* 21 (2011):3-4.

34. Isom, L.L., W.A. Catterall. “Na+ channel subunits and Ig domains.” *Nature* 383.6598(1996):307-308.

35. Isom, L.L., K.S. De Jongh, D.E. Patton, B.F. Reber, J. Offord, H. Charbonneau, K. Walsh, A.L. Goldin, W.A. Catterall. “Primary structure and functional expression of the beta 1 subunit of the rat brain sodium channel.” *Science* 256.5058 (1992):839-842.

36. Isom, L.L., D.S. Ragsdale, K.S. De Jongh, R.E. Westenbroek, B.F. Reber, T. Scheuer, W.A. Catterall. “Structure and function of the beta 2 subunit of brain sodium channels, a transmembrane glycoprotein with a CAM motif.” *Cell* 83.3 (1995):433-442.

37. Jao, Li-En., S.R. Wente, and W. Chen. (2013) “Efficient multiplex biallelic zebrafish genome editing using a CRISPR nuclease system.” *Proceedings of the National Academy of Sciences* 110.34 (2013):13904-13909.

38. Jinek, M., K. Chylinski, I. Fonfara, M. Hauer, J.A. Doudna. “A programmable dual-RNA-guided DNA endonuclease in adaptive bacterial immunity.” *Science* 337.6096(2012):816–821.

39. Joung and Sander. “TALENs: a widely applicable technology for targeted genome editing.” *Nature* 14(2013):49-55.

40. Kawaguchi, M., H. Takahashi, Y. Takehana, K. Naruse, M. Nishida, S. Yasumasu. “Sub-functionalization of duplicated genes in the evolution of nine-spined stickleback hatching enzyme.” *Journal of Experimental Zoology Part B Molecular and Developmental Evolution* 320B (2013): 140-150.

41. Keating, M.T. “The long QT syndrome. A review of recent molecular genetic and physiologic discoveries.” *Medicine (Baltimore)* 75.1(1996):1-5.

42. Kersey, P.J., et al*. Ensembl Genomes 2013: scaling up access to genome-wide data Nucleic acids research* 42.D1 (2013): D546-D552.

43. Koopmann, T.T., C.R. Bezzina, A.A. Wilde. “Voltage-gated sodium channels: action players with many faces.” Annals of Internal Medicine 38.7 (2006):472-482.

44. Kyndt, F., V. Probst, F. Potet, S. Demolombe, J-C. Chevallier, I. Baro, et al. “Novel *SCN5A* Mutation Leading Either to Isolated Cardiac Conduction Defect or Brugada Syndrome in a Large French Family.” *Circulation* 104(2001):3081-3086.

45. Lambert, M.J., W.O. Cochran, B.M. Wilde, K.G. Olsen, C.D. Cooper. “Evidence for widespread subfunctionalization of splice forms in vertebrate genomes.” *Genome Research* 25(2015):114-120.

46. Lehmann-Horn, F., K. Jurkat-Rott. “Voltage-Gated Ion Channels and Hereditary Disease.” *Physiological Reviews* 79.4 (1999):1317-1372.

47. Lei, M., C. Goddard, J. Liu, A.L. Léoni, A. Royer, S.S. Fung, G. Xiao, A. Ma, H. Zhang, F. Charpentier, J.I. Vandenberg, W.H. Colledge, A.A. Grace, C.L. Huang. “Sinus node dysfunction following targeted disruption of the murine cardiac sodium channel gene *Scn5a*.” *Journal of Physiology* 567.Pt 2 (2005):387-400.

48. Liu, H., M. Tateyama, C.E. Clancy, H. Abriel, R.S. Kass. “Channel openings are necessary but not sufficient for use-dependent block of cardiac Na(+) channels by flecainide: evidence from the analysis of disease-linked mutations.” *Journal of General Physiology* 120.1(2002):39-51.

49. Machlis, G.E., M.K. McNutt. “Disasters. Scenario-building for the Deepwater Horizon oil spill.” *Science* 329 (2010):1018-1019.

50. Marban, E., T. Yamagishi, G.F. Tomaselli. “Structure and function of voltage-gated sodium channels.” *Journal of Physiology* 508.Pt 3(1998):647-657.

51. Marban, E. “Cardiac channelopathies.” *Nature* 415.6868(2002):213-218.

52. Mohler, P.J., J.J. Schott, A.O. Gramolini, K. W. Dilly, S. Guatimosim, W. H. duBell, L-S. Song, K. Haurogné, F. Kyndt, M. E. Ali, T. B. Rogers, W. J. Lederer, D. Escande, H. L. Marec, and V. Bennett. “Ankyrin-B mutation causes type 4 long-QT cardiac arrhythmia and sudden cardiac death.” *Nature* 421.6923(2003):634-639.

53. Morgan, K., E.B. Stevens, B. Shah, P.J. Cox, A.K. Dixon, K. Lee, R.D. Pinnock, J. Hughes, P.J. Richardson, K. Mizuguchi, A.P. Jackson. “Beta 3: an additional auxiliary subunit of the voltage-sensitive sodium channel that modulates channel gating with distinct kinetics.” *Proceedings of the National Academy of Sciences (USA)* 97.5(2000):2308-2313.

54. Moss, A.J., “Long QT Syndrome.” *Journal of the American Medical Association* 289.16(2003):2041-2044.

55. Nebert, D.W., T.P. Dalton, A.B. Okey, F.J. Gonzalez. “Role of aryl hydrocarbon receptor-mediated induction of the CYP1 enzymes in environmental toxicity and cancer.” *Journal of Biological Chemistry* 279(2004):23847–23850.

56. Novak, A.E., A.D. Taylor, R.H. Pineda, E.L. Lasda, M.A. Wright, A.B. Ribera. “Embryonic and larval expression of zebrafish voltage-gated sodium channel alpha-subunit genes.” *Developmental Dynamics* 235.7(2006):1962-73.

57. Novak, A.E., M.C. Jost, Y. Lu, A.D. Taylor, H.H. Zakon, A.B. Ribera. “Gene duplications and evolution of vertebrate voltage-gated sodium channels.” *Journal of Molecular Evolution* 63(2006):208-21.

58. Nuyens, D., M. Stengl, S. Dugarmaa, et al. “Abrupt rate accelerations or premature beats cause life-threatening arrhythmias in mice with long-QT3 syndrome.” *Nature Medicine* 7.9(2001):1021-1027.

59. Papadatos, G.A., P.M. Wallerstein, C.E. Head, R. Ratcliff, P.A. Brady, K. Benndorf, R.C. Saumarez, A.E. Trezise, C.L. Huang, J.I. Vandenberg, W.H. Colledge, A.A. Grace. “Slowed conduction and ventricular tachycardia after targeted disruption of the cardiac sodium channel gene *Scn5a*.” *Proceedings of National Academy of Sciences (USA)* 99.9(2002):6210-6215.

60. Pauka, L.M., M. Maceno, S.C. Rossi, S.H. de Assis. “Embryotoxicity and biotransformation responses in zebrafish exposed to water-soluble fraction of crude oil.” *Bulletin of Environmental and Contamination Toxicology* 86(2011):389-393.

61. Postlethwait, J., A. Amores, W. Cresko, A. Singer, Y.L. Yan. “Subfunction partitioning, the teleost radiation and the annotation of the human genome.” Trends Genet (2004).

62. Pu, J., J.R. Balser, P.A. Boyden. “Lidocaine action on Na+ currents in ventricular myocytes from the epicardial border zone of the infarcted heart.” *Circulation Research* 83.4(1998):431-440.

63. Reyon, D., S.Q. Tsai, C. Khayter, J.A. Foden, J.D. Sander, and J.K. Joung. “FLASH assembly of TALENs for high-throughput genome editing.” *Nature Biotechnology* 30 (2012):460–465.

64. Ribera, A.B., C. Nusslein-Volhard. “Zebrafish touch-insensitive mutants reveal an essential role for the developmental regulation of sodium current.” *Journal of Neuroscience* 18.22(1998):91819191.

65. Roden, D.M., J.R. Balser, A.L. George, M.E. Anderson Jr. “Cardiac ion channels.” *Annual Review of Physiology* 64 (2002):431-475.

66. Rogart, R.B., L.L. Cribbs, L.K. Muglia, D.D. Kephart, M.W. Kaiser. “Molecular cloning of a putative tetodotoxin-resistant rat heart Na+ channel isoform.” *Proceedings of the National Academy of Sciences* (1989).

67. Rosen, J.N., M.F. Sweeney, J.D. Mably. “Microinjection of zebrafish Embryos to Analyze Gene Function.” *Journal of Visualized Experiment* 25 (2009).

68. Shimizu W., C. Antzelevitch, K. Suyama, T. Kurita, A. Taguchi, N. Aihara, H. Takaki, K. Sunagawa, S. Kamakura. “Effect of sodium channel blockers on ST segment, QRS duration, and corrected QT interval in patients with Brugada syndrome.” *Journal of Cardiovascular Electrophysiology* 11.12(2000):1320-1329.

69. Sun, Y-M., I. Favre, L. Schild, E. Moczydlowsk. “On the Structural Basis for Size-selective Permeation of Organic Cations through the Voltage-gated Sodium Channel-Effect of Alanine Mutations at the DEKA Locus on Selectivity, Inhibition by Ca2+ and H+, and Molecular Sieving” Journal of General Physiology 110.6 (1997):693-715.

70. Tsai, C.W., J.J. Tseng, S.C. Lin, C.Y. Chang, J.L. Wu, J.F. Horng, H.J. Tsay. “Primary structure and developmental expression of zebrafish sodium channel Na(v)1.6 during neurogenesis.” *DNA and Cell Biology* 20.5 (2001):249255.

71. "Using PubMed." *National Center for Biotechnology Information*. U.S. National Library of Medicine. Web. 10 Apr. 2013. http://www.ncbi.nlm.nih.gov/pubmed/

72. Valdivia, C.R., D.J. Tester, B.A. Rok, C.B. Porter, T.M. Munger, A. Jahangir, J.C. Makielski, M.J. Ackerman. “A trafficking defective, Brugada syndrome-causing *SCN5A* mutation rescued by drugs.” *Cardiovascular Research* 62.1(2004):53-62.

73. Vatta, M., R. Dumaine, C. Antzelevitch, R. Brugada, H. Li, N.E. Bowles, K. Nademanee, J. Brugada, P. Brugada, J.A. Towbin. “Novel mutations in domain I of *SCN5A* cause Brugada syndrome.” *Molecular Genetics and Metabolism* 75.4(2002):317-324.

74. Vincent, G.M. “The molecular genetics of the long QT syndrome: genes causing fainting and sudden death.” *Annual Review of Medicine* 49(1998):263-74.

75. Viswanathan, P.C., C.R. Bezzina, A.L. George, D.M. Roden Jr., A.A. Wilde, J.R. Balser. “Gatingdependent mechanisms for flecainide action in *SCN5A*-linked arrhythmia syndromes.” *Circulation* 104.10(2001):1200-1205.

76. Wang, D.W., N. Makita, A. Kitabatake, J.R. Balser, A.L. George Jr. “Enhanced Na(+) channel intermediate inactivation in Brugada syndrome.” *Circulation Research* 87.8(2000):E37-E43.

77. Wang, D.W., K. Yazawa, A.L. George, P.B. Bennett Jr. “Characterization of human cardiac Na+ channel mutations in the congenital long QT syndrome.” *Proceedings of the National Academy Sciences (USA)* 1996; 93.23(1996):13200-13205.

78. Wang, Q., Z. Li, J. Shen, M.T. Keating. “Genomic organization of the human *SCN5A* gene encoding the cardiac sodium channel.” *Genomics* 34.1(1996):9-16.

79. Wang, Q., J. Shen, I. Splawski, D. Atkinson, Z. Li, J.L. Robinson, A.J. Moss, J.A. Towbin, M.T. Keating. "*SCN5A* mutations associated with an inherited cardiac arrhythmia, long QT syndrome." *Cell* 80.5(1995):805-811.

80. Wang, Q., S. Chen, Q. Chen, X. Wan, J. Shen, G. A. Hoeltge, A. A. Timur, M. T. Keating, G. E. Kirsch. "The common SCN5A mutation R1193Q causes LQTS-type electrophysiological alterations of the cardiac sodium channel." *Journal of Medical Genetics* 41.e66(2004).

81. Warren, K.S., K. Baker, M.C. Fishman. "The slow mo mutation reduces pacemaker current and heart rate in adult zebrafish." *Heart and Circulatory Physiology* 281.4(2001):H1711-H1719.

82. Watanabe, E., A. Fujikawa, H. Matsunaga H, Y. Yasoshima, N. Sako, T. Yamamoto, C. Saegusa , M. Noda. "Nav2/NaG channel is involved in control of salt-intake behavior in the CNS." *Journal of Neuroscience* 20.20(2000):7743-7751.

83. Yu, F.H., W.A. Catterall. "Overview of the voltage-gated sodium channel family." *Genome Biology* 4.3(2003):207.

84. Yu, FH., R.E. Westenbroek, I. Silos-Santiago, K.A. McCormick, D. Lawson, P. Ge, H. Ferriera, J. Lilly, P.S. DiStefano, W.A. Catterall, T. Scheuer, R. Curtis. "Sodium channel beta4, a new disulfidelinked auxiliary subunit with similarity to beta2." *Journal of Neuroscience* 23.20(2003):7577-7585.

85. Zipes, D.P., H.J. Wellens. "Sudden cardiac death." *Circulation* 98.21(1998):2334-2351.

APPENDIX A-1: IACUC PI Approval Letter to Work with zebrafish

East Carolina University

Animal Care and Use Commitee
212 Ed Warren Life Sciences Building
East Carolina University
Greenville, NC 27834

252-744-2436 office
252-744-2355 fax

February 6, 2014

Yong Zhu, Ph.D.
Department of Biology
Howell Science Complex
East Carolina University

Dear Dr. Zhu:

Your Animal Use Protocol entitled, "Studies of Hormones and Receptors in Zebrafish" (AUP #D185d) was reviewed by this institution's Animal Care and Use Committee on 2/6/14. The following action was taken by the Committee:

"Approved as submitted"

Please contact Dale Aycock at 744-2997 prior to hazard use

A copy is enclosed for your laboratory files. Please be reminded that all animal procedures must be conducted as described in the approved Animal Use Protocol. Modifications of these procedures cannot be performed without prior approval of the ACUC. The Animal Welfare Act and Public Health Service Guidelines require the ACUC to suspend activities not in accordance with approved procedures and report such activities to the responsible University Official (Vice Chancellor for Health Sciences or Vice Chancellor for Academic Affairs) and appropriate federal Agencies. **Please ensure that all personnel associated with this protocol have access to this approved copy of the AUP and are familiar with its contents.**

Sincerely yours,

Susan McRae, Ph.D.
Chair, Animal Care and Use Committee

SM/jd

Enclosure

Appendix A-2: Animal Use Protocol Form

EAST CAROLINA UNIVERSITY
ANIMAL USE PROTOCOL (AUP) FORM
LATEST REVISION NOVEMBER, 2013

Project Title:
Studies of Hormones and Receptors in Zebrafish

	Principal Investigator	Secondary Contact
Name	Yong Zhu	Edmund J Stellwag
Dept.	Biology	Biology
Office Ph #	252-328-6504	252-328-6302
Cell Ph #	252-439-0288	Click here to enter text.
Pager #	Click here to enter text.	Click here to enter text.
Home Ph #	Click here to enter text.	Click here to enter text.
Email	zhuy@ecu.edu	stellwage@ecu.edu

For IACUC Use Only

AUP # D185d			
New/Renewal Renewal 2/6/14			
Full Review/Date	DR/Date		
Approval Date 2/6/14			
Study Type hormones + embryo development			
Pain/Distress Category C			
Surgery	Survival	Multiple	
Prolonged Restraint			
Food/Fluid Regulation			
Other			
Hazard Approval/Dates	Rad	IBC ✓ e mail 12/13/13	EHS ✓ 1/28/14
OHP Enrollment			17a, 20-Dihydroxy 4-pregnen-3-one,
Mandatory Training			
Amendments Approved			B estradiol

Exception to Guide: 10 adult fish/liter instead of 5

APPENDIX A-3: List of Personnel working with zebrafish

I. Personnel

A. Principal Investigator(s):
Yong Zhu

B. Department(s):
Biology

C. List all personnel (PI's, co-investigators, technicians, students) that will be working with live animals and describe their qualifications and experience with these specific procedures. If people are to be trained, indicate by whom:

Name/Degree/Certification	Position/Role(s)/ Responsibilities in this Project	Required Online IACUC Training (Yes/No)	Relevant Animal Experience/Training (include species, procedures, number of years, etc.)
Yong Zhu/PhD	Associate Professor/PI/Supervisor	Yes	Have relevant animal experience and training with fish since 1986, know well zebrafish husbandry requirements, spawning protocol, and microinjection procedure etc., responsible for training all associates working in the lab
Edmund J Stellwag/PhD	Associate Professor/Co-investigator/co-supervisor	Yes	Over 20 yrs with fish, 10 yrs with zebrafish, helping training associates
Jeffery McKinnon/PhD	Professor/Co-Investigator/co-supervisor	Yes	Over 20 yrs with fish, helping training associates
Zoe C Shaner	PhD Student/student	Yes	One year with zebrafish, train directly by PI (Zhu)
Lengxob Yong	PhD Candidate/Student	Yes	10 years with fish, one year with zebrafish, train by PIs (Mcknnon & Zhu)
Payal M Chokshi	MS student/Student	Yes	One year with zebrafish, train by PIs (Stellwag & Zhu)
Tsewntoo Thao	Undergraduate/Student	Yes	One year with zebrafish, train by PI and graduate student (Zhu & Yong)
Zayer Thet	Undergraduate/Student	Yes	One year with zebrafish, train by PI and a graduate student (Zhu & Shaner)
Avian White	Undergraduate/Student	Yes	6 months with zebrafish, train by PI and a graduate student

APPENDIX A-4: Approval of Working with Transgenic Zebrafish

C. Hazardous Agents

1. **Protocol related hazards (chemical, biological, or radiological):**
   Please indicate if any of the following are used in animals and the status of review/approval by the referenced committees:

HAZARDS	Oversight Committee	Status (Approved, Pending, Submitted)/Date	AUP Appendix I Completed?
Radioisotopes	Radiation	Click here to enter text.	Choose an item.
Ionizing radiation	Radiation	Click here to enter text.	Choose an item.
Infectious agents (bacteria, viruses, rickettsia, prions, etc.)	IBC	Click here to enter text.	Choose an item.
Toxins of biological origins (venoms, plant toxins, etc.)	IBC	Click here to enter text.	Choose an item.
Transgenic, Knock In, Knock Out Animals---breeding, cross breeding or any use of live animals or tissues	IBC	Has been approved/12/13/2013	Yes
Human tissues, cells, body fluids, cell lines	IBC	Has been approved/12/13/2013	Yes

5

Viral/Plasmid Vectors/Recombinant DNA or recombinant techniques	IBC	Has been approved/12/13/2013	Yes
Oncogenic/toxic/mutagenic chemical agents	EH&S	Click here to enter text.	Choose an item.
Nanoparticles	EH&S	Click here to enter text.	Choose an item.
Cell lines, tissues or other biological products injected or implanted in animals	DCM	Click here to enter text.	Choose an item.
Other agents		Click here to enter text.	Choose an item.

APPENDIX A-5: Final IACUC Approval

I acknowledge that humane care and use of animals in research, teaching and testing is of paramount importance, and agree to conduct animal studies with professionalism, using ethical principles of sound animal stewardship. I further acknowledge that I will perform only those procedures that are described in this AUP and that my use of animals must conform to the standards described in the Animal Welfare Act, the Public Health Service Policy, The Guide For the Care and Use of Laboratory Animals, the Association for the Assessment and Accreditation of Laboratory Animal Care, and East Carolina University.

Please submit the completed animal use protocol form via e-mail attachment to iacuc@ecu.edu. You must also carbon copy your Department Chair.

PI Signature: Yong Zhu email ✓ Date: 2-6-2014

Veterinarian: Karen A. Oppelt Date: 2/6/14

IACUC Chair: S B McRae jr Date: 2/6/14

APPENDIX B: Developmental defects observed by Chopra et al. in zebrafish MOs.

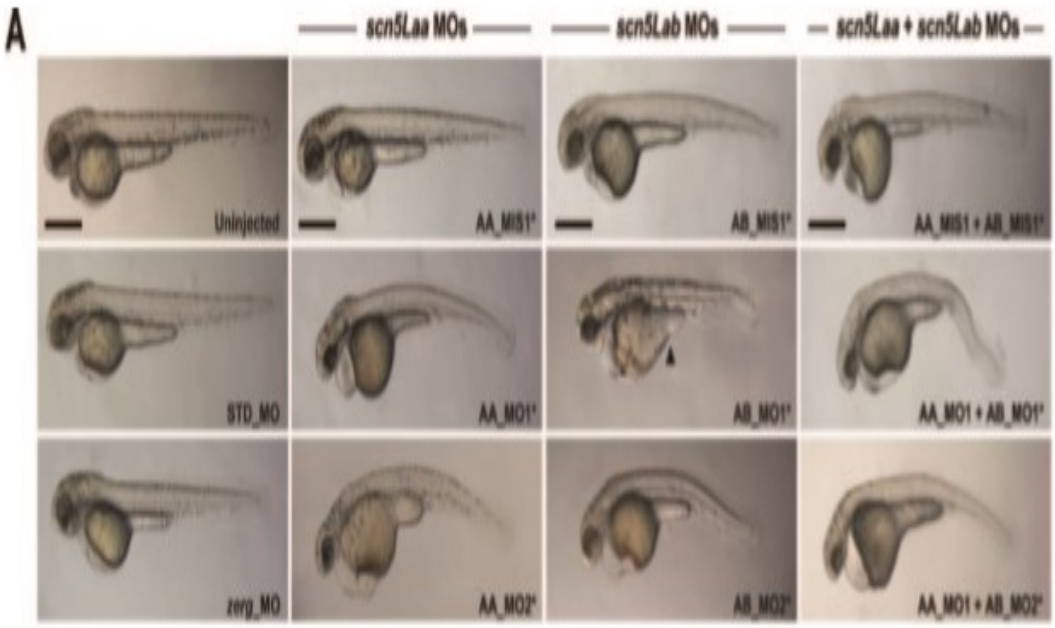

Above embryos show various developmental defects due to knockdown of either *scn5Laa* or *scn5Lab*. These morpholinos show cardiac edema, yolk sac edema, curvature of spine, abnormal cardiac development, LQTS, Bradycardia, Sudden cardiac death syndrome, etc. compared to uninjected embryos. Developmental defects are severe in the embryos injected with both *scn5Laa* and *scn5Lab* morpholinos (Chopra et al. 2010).

APPENDIX C: The effects of crude oil derivities on embryonic development of zebrafish (de Soysa et al. 2010)

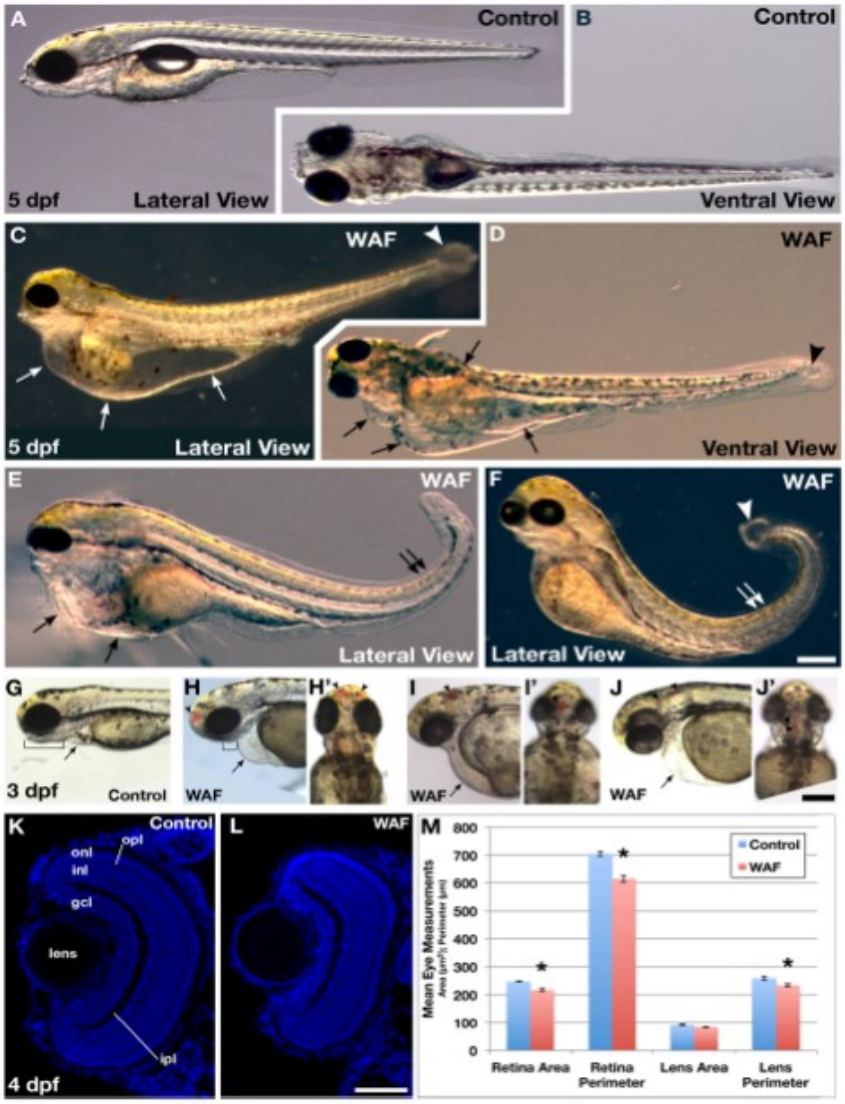

Figure 1 Exposure to Macondo crude oil-derived WAFs induced diverse gross morphological deformations in zebrafish embryos. (**A-F**) Lateral and ventral views of live untreated control (A, B) and WAF-treated embryos (C-F) at 5 dpf. Severe cardiac and yolk edema (C, D, E, arrows), dorsal tail curvature (E, F, double arrows), and cysts at the tip of the tail (C, D, F, arrowhead) were visible. (**G, H**) WAF-treated embryos (H) had reduced jaws compared to controls (G, brackets). (G-**J**) At 3 dpf cardiac edema was evident in WAF-treated embryos (arrows), and 28% of embryos had hemorrhaging in the forebrain, midbrain and hindbrain (arrowheads). Lateral (G, H, I, J) and dorsal views (H', I', J'). (**K-M**) Retinal architecture appeared normal in control and WAF-treated embryos (K, L) but there was a slight reduction in the area and perimeter of WAF-treated retinas (M). Except for lens area, the size reductions were statistically significant (M, asterisks; *t*-tests: lens area, $P = 0.015$; lens perimeter, $P = 0.007$; retina area $P < 0.0005$; retina perimeter, $P < 0.0005$). Scale bars: 200 μm, F, J'; 50 μm, L. Abbreviations: gcl, ganglion cell layer; ipl, inner plexiform layer; inl, inner nuclear layer; opl, outer plexiform layer; onl. outer nuclear layer.